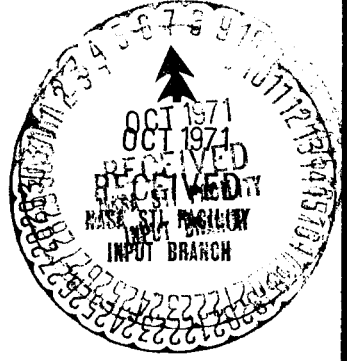
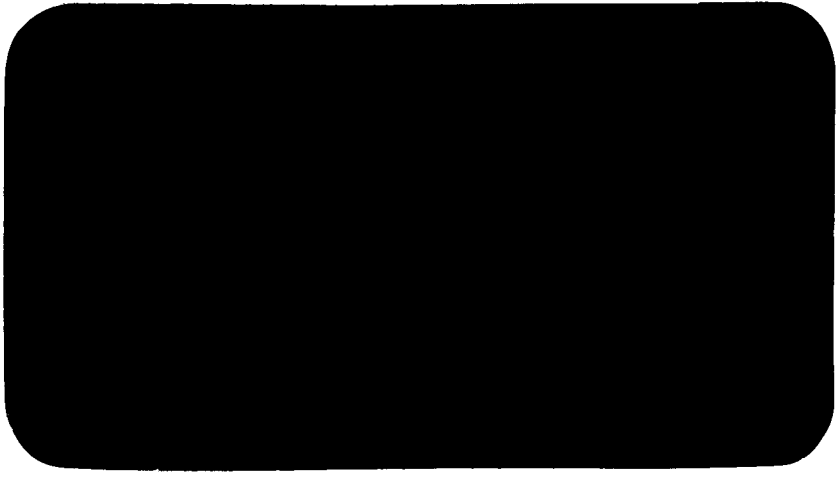


1/P
Hester



N72-13366 (NASA-CR-124810) DEVELOPMENT OF A POSITION SENSITIVE X-RAY DETECTOR FOR USE IN A LIGHT WEIGHT X-RAY DIFFRACTOMETER Final Report, 1 Aug. 1970 - 31 R.A. Semmler (IIT Research Inst.) Jul. 1971 60 p CSCL 14B G3/14

Unclas 10926

(NASA CR OR TMA OR AD NUMBER) (CATEGORY)

Ri

60

Contract No. NASW-2111
Report No. IITRI-V6112-4

DEVELOPMENT OF A POSITION SENSITIVE
X-RAY DETECTOR FOR USE IN A LIGHT
WEIGHT X-RAY DIFFRACTOMETER

NASA Headquarters
Washington, D. C. 20546

Attention: Dr. Robert Bryson
Code MAL

Prepared by

R. A. Semmler

IIT Research Institute
10 West 35th Street
Chicago, Illinois 60616

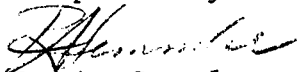
July 1971

Final Report for Period August 1, 1970
Through July 31, 1971

FOREWORD

This is the final report under Contract No. NASW-2111 covering the period from August 1, 1970 through July 31, 1971. This project continues the development work on position sensitive counters initiated under internal research projects V1000 and V1037. Project data is contained in Logbook C19792.

Prepared by



R. A. Semmler
Research Physicist
Nuclear and Radiation Physics

Approved by



C. A. Stone, Director
Physics Research Division

/gjd

Preceding page blank

TABLE OF CONTENTS

	<u>Page</u>
1. SUMMARY AND RECOMMENDATIONS	1
2. INTRODUCTION	3
3. DETECTOR DEVELOPMENT	6
4. ELECTRONIC SYSTEM	11
5. EXPERIMENTAL RESULTS: QUARTZ DIFFRACTION WITH THE 137° COUNTER	16
5.1 Energy Resolution	21
5.2 Sensitivity	21
6. ANCILLARY STUDIES	22
6.1 Slant Path Effects	22
6.2 Anode Support Systems	31
6.3 Pure Carbon Anodes	34
6.4 Resolution Limitations	36
6.5 0.1 Percent Analogue Divider Tests	39
7. REFERENCES	41
APPENDIX A - DRAWINGS FOR THE 137° COUNTER	43
APPENDIX B - COMPUTER PROGRAM LISTINGS AND SAMPLE EXECUTIONS	49

DEVELOPMENT OF A POSITION SENSITIVE X-RAY DETECTOR FOR USE IN A LIGHT WEIGHT X-RAY DIFFRACTOMETER

1. SUMMARY AND RECOMMENDATIONS

The motivation for the development of a position sensitive proportional counter for use in an X-ray diffractometer is the promise of a detector which is efficient enough to permit drastic reductions in the power and weight requirements of the X-ray source and the elimination of the power, weight and complexity of a moving slit. Significant progress toward this goal through the demonstration of the application of such a counter in an X-ray diffractometer has been achieved during this contract. The final detector constructed and tested has a window spanning 138° and a free standing anode curved along an arc of 7.1 cm radius. Demonstration spectra of a quartz sample in a Debye-Sherrer geometry indicate a spatial resolution of 0.4 - 0.5 mm ($0.3^\circ - 0.4^\circ 2\theta$). The present detector is about 30 times faster than film and is estimated to be 300 times more efficient than a scanning slit system. It would require an X-ray source with a power consumption of about 1 watt. By comparison, the lunar diffractometer consumed 25 watts in the X-ray generator and weighed about 20 pounds. The elimination of moving parts and the reduction in size of the X-ray power supply leads to the expectation of a diffractometer that could have a mass as small as 6 pounds.

During this project the primary problems encountered were the result of non-uniformity of the anode wire, an experimental product from an outside vendor. Improvement of anode quality by better control of the fabrication process, use of more uniform raw materials, or use of different fabrication techniques should be examined. This is expected to be a relatively straightforward step.

The present work was limited to a non-focusing (Debye-Sherrer) geometry; however, a focusing geometry is essential if the maximum gain in efficiency is to be fully realized.

In a focusing geometry the slant path effect causes a significant loss in spatial resolution. A partial solution is to reduce the path length by employing a high atomic number gas at elevated pressure. With xenon at 2 atmospheres pressure, the spatial resolution will be about 1 mm ($\sim 0.8^\circ$) for paths making an angle less than 45° with the anode. This figure can be further reduced using deconvolution techniques.

As implied in the above paragraphs, the practical feasibility of using the position sensitive proportional counter to obtain a quality diffraction pattern in a standard geometry has been demonstrated. Future efforts are to be directed toward the goal of a counter coupled with a diffractometer which could ultimately be developed for remote application. As part of this program the following steps need to be taken:

1. Evaluate a detector in a focusing geometry.
2. Develop a detector which is sealed permitting the use of xenon at elevated pressure.
3. Evaluate the X-ray fluorescence analysis capabilities of such an instrument.
4. Provide improved anode wires.

2. INTRODUCTION

This is the final report on the development of a curved position sensitive detector suitable for use with X-ray diffraction apparatus. This program is a continuation of work initiated under internally sponsored feasibility studies. (1,2,3)

All detectors constructed thus far have been gas filled proportional counters with a single resistive anode. Position is determined by comparing the amplitude of the signals at each end of the wire.

The status at the beginning of this program is best indicated by the actual diffraction patterns displayed in Figs. 1 and 2. Conventional film techniques result in the pattern shown in Fig. 1; the position sensitive counter result is in Fig. 2. The experimental conditions are in Table 1 and 2. As noted in Table 2, the spectra shown in Fig. 2 is a composite spectrum formed from 6 separate spectra obtained with a curved 17° detector.

The primary purpose of the present program was to achieve diffraction spectra comparable to Fig. 1 using a single wide angle detector. This has been successfully accomplished.

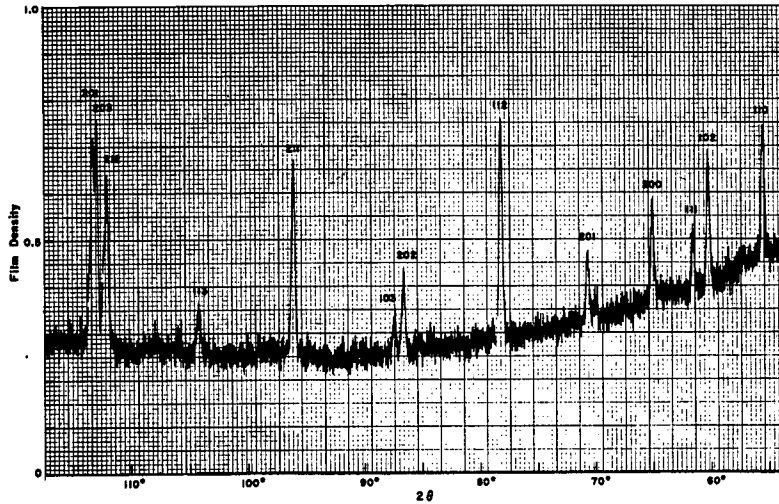


Figure 1 QUARTZ DIFFRACTION PATTERN USING KODAK NO-SCREEN FILM WITH GE POWDER CAMERA. 3 hour exposure (35 kV, 25 ma, Cr radiation).

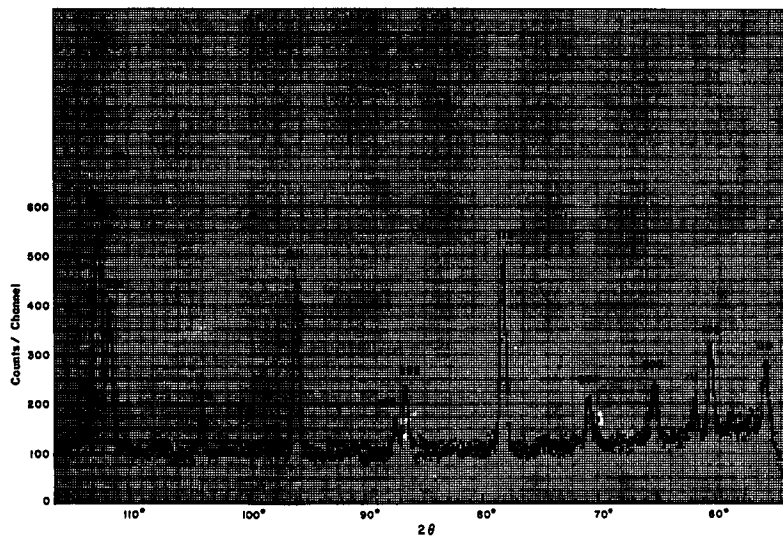


Figure 2 QUARTZ DIFFRACTION PATTERN USING POSITION-SENSITIVE DETECTOR WITH GE POWDER CAMERA. Composite of 6 overlapping spectra of 15° each. 10 minute exposure each. (35 kV, 25 ma, Cr radiation)

Table 1
EXPERIMENTAL CONDITIONS FOR THE FILM EXPOSURE

Geometry:	GE XRD powder camera with 7.16 cm film radius
Film:	Kodak no-screen X-ray film
Development:	5 min. in GE Supermix Developer
Sample:	Pulverized Ottawa sand
Sample holder:	0.3 mm capillary
Sample rotation:	1 rpm
Collimation:	0.4 x 2.5 mm slit
X-ray tube:	CA-7H with chromium target, vanadic acid filter
X-ray tube voltage:	35,000 V
X-ray tube current:	25 ma
Exposure time:	3 hours

Table 2
EXPERIMENTAL CONDITIONS FOR THE POSITION SENSITIVE PROPORTIONAL COUNTER EXPOSURE

Geometry:	GE XRD powder camera with position sensitive counter mounted instead of film. Anode wire radius is 7.46 cm (2-15/16 in.)
Sample:	Pulverized Ottawa sand
Sample holder:	0.3 mm capillary
Sample rotation:	1 rpm
Collimation:	0.4 x 2.5 mm slit
X-ray tube:	CA-7H with chromium target, canadic acid filter
X-ray tube voltage:	35,000 V
X-ray tube current:	25 ma
Exposure time:	10 min. each (6 overlapping 15° spectra)

3. DETECTOR DEVELOPMENT

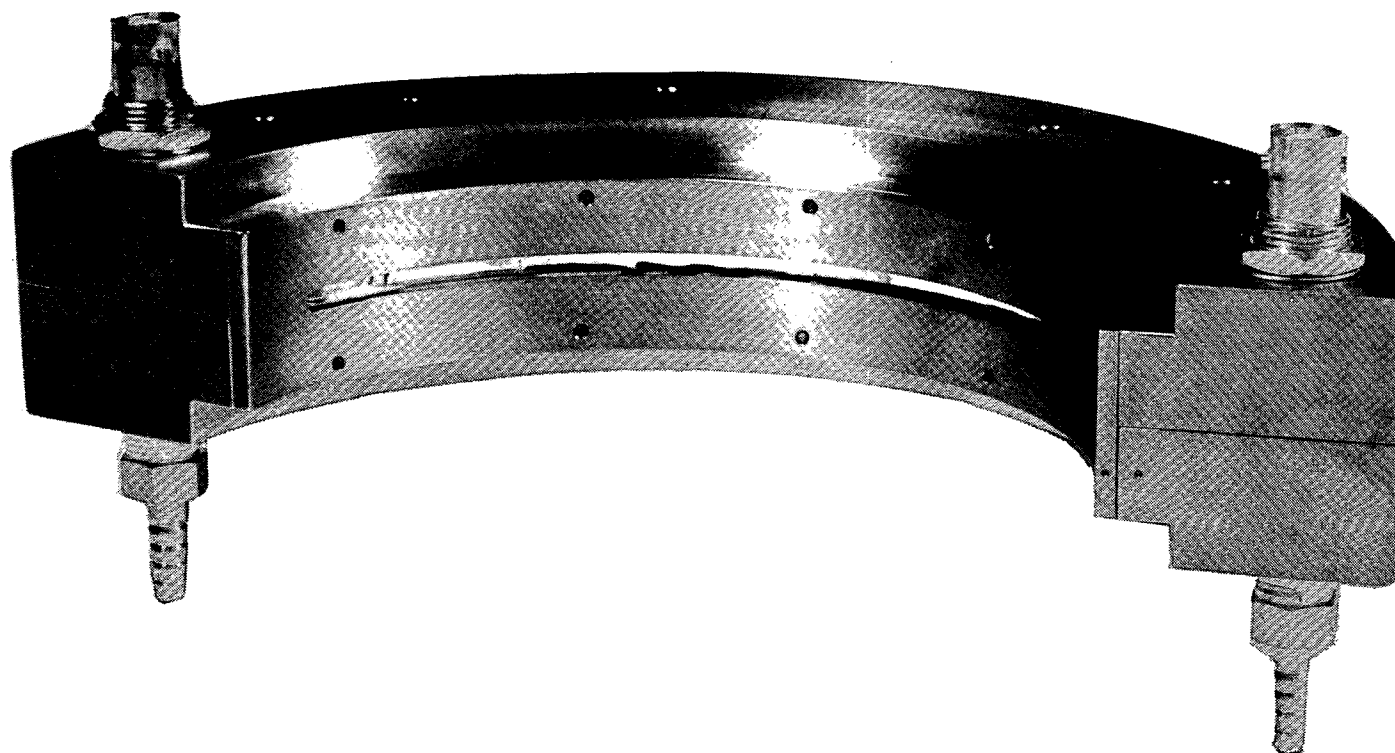
A curved (137° window) proportional counter with support points only at the ends of the anode wire, was designed and constructed during this contract. Like the earlier short arc counter, this counter fits a General Electric powder diffraction camera but has a much longer window and a heavier (5 mil) anode. The assembled counter is shown by itself and mounted on a GE camera in Figs. 3 and 4.

The counter has a circular cross section $1/2$ inch in diameter, and is operated with conventional P-10 counting gas. The anode is not soldered but is clamped between soft conductive gaskets to facilitate replacement and adjustment of anode position within the counter (see Appendix A).

The first anode mounted was a 4 mil free standing stainless steel (SS) wire. (One mil wire such as used in the 17° counter is not sufficiently rigid to span the 147° between end supports.) Satisfactory proportional operation was achieved (< 20 percent resolution for Fe-55) with this free standing wire over the range 1600-1900 volts.

The SS wire was then replaced with a 5 mil quartz fiber coated with pyrolytic carbon - again free standing between the end support points. With care, proportional operation was achieved with this free standing anode up to 2225 volts. At this point, the anode was pulled to the wall.

An example of the position resolution obtained with the 5 mil anode is shown in Fig. 5. This is an expanded view of a small portion of the wire and was obtained using a 4-slit collimator and an Fe-55 source. The resolution (FWHM) of the central peaks is approximately 0.4 mm. The contributions to this width are approximately 0.22 mm from the slit itself, 0.25 mm from the electronic noise, and 0.28 mm (balance) from the inherent detector resolution.



7

Figure 3 VIEW OF THE 137° COUNTER FROM THE WINDOW SIDE.
(Anode radius is 2-13/16".)

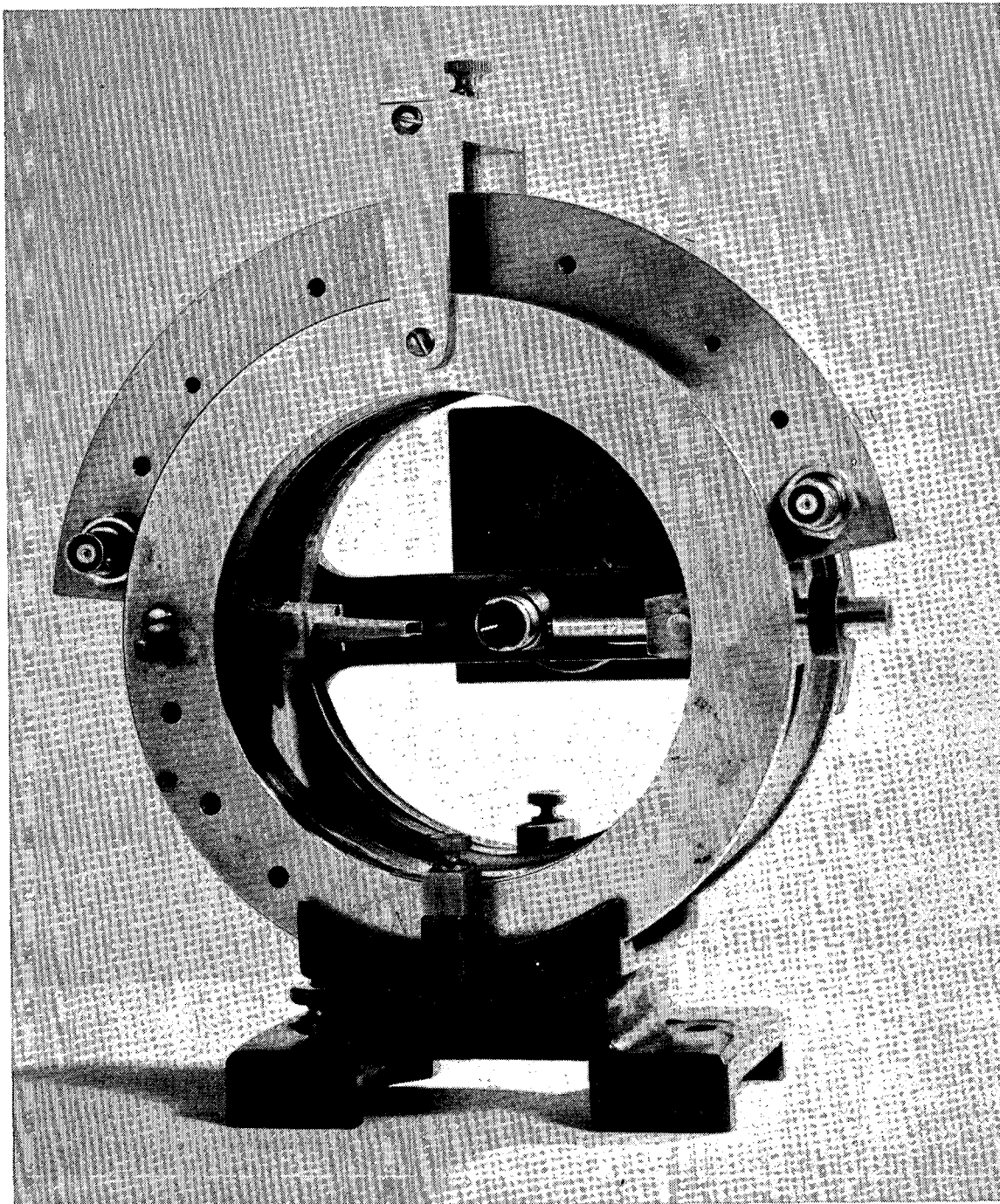


Figure 4

VIEW OF THE 137° COUNTER MOUNTED ON A GE
POWDER DIFFRACTION CAMERA.

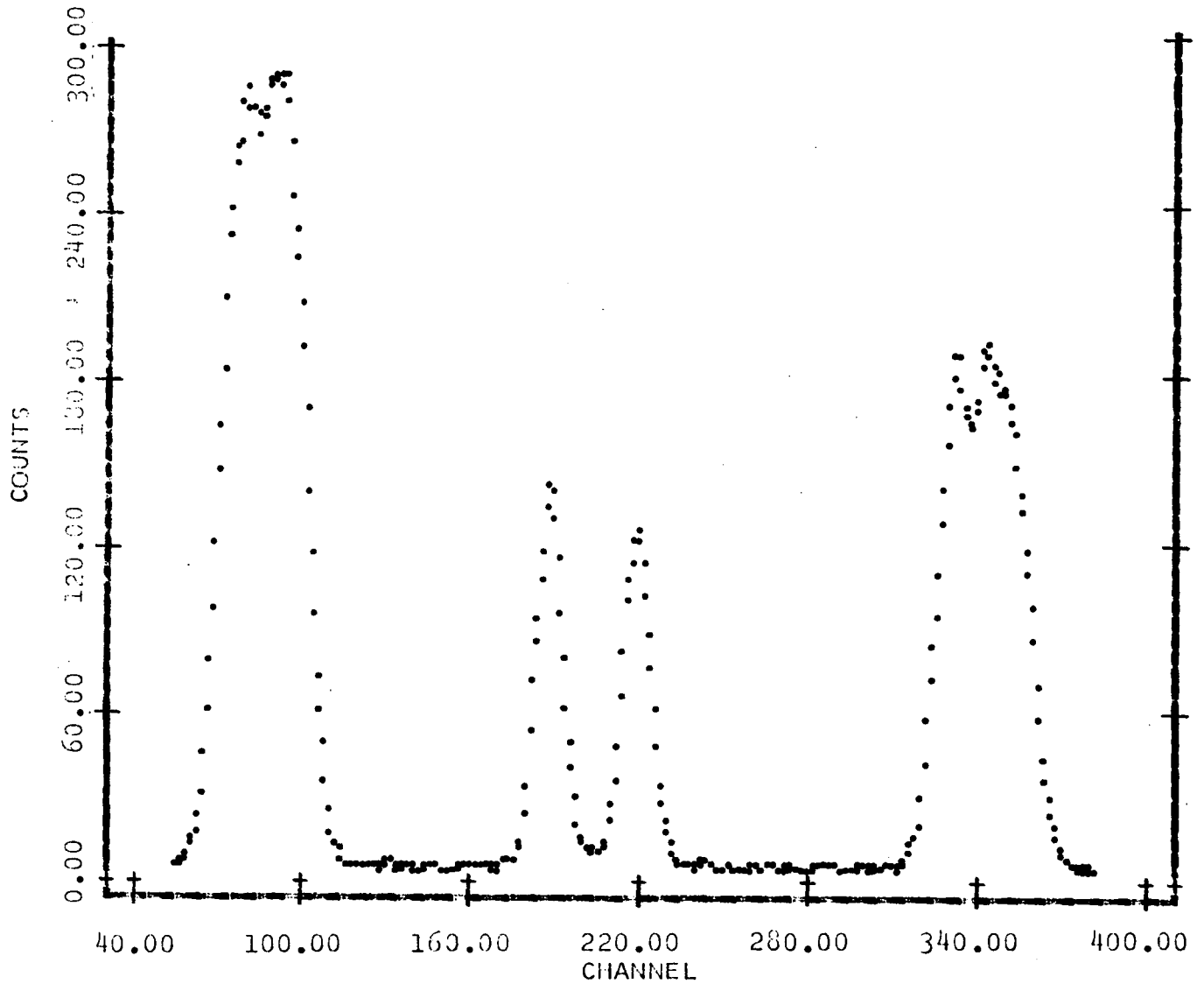


Figure 5 POSITION SPECTRUM USING A FOUR-SLIT COLLIMATOR IN FRONT OF THE 137° DETECTOR WITH A 5 MIL ANODE. The central pair of peaks is generated by slits 0.22 mm wide separated by 1.1 mm. (Data has been smoothed with a 7 point quadratic piecewise polynomial.)

The energy resolution with the 5 mil anode was unexpectedly poor compared to the previous experience with a 1 mil anode. The best resolution for Fe-55 was only about 20 percent; 30 percent was a more typical figure. Both the gas gain and resolution varied with position. It is not known whether this variation is caused by surface irregularities, ellipticity in the fiber, or other unknown factors.

A set of reduced size drawings for the 137° counter is included in Appendix A.

4. ELECTRONIC SYSTEM

Position is determined from the counter by charge division and the electronic system is designed to measure the ratio $Q_1/(Q_1 + Q_2)$, where Q_1 and Q_2 are the charges collected at each end of the anode wire in the position sensitive counter.

A block diagram of the electronic system is shown in Fig. 6. The actual components used in the system are listed in Table 3. The actual pulses as they appear in the system are shown in Fig. 7.

Subsequent changes included a reduction in preamp bandwidth to eliminate preamplifier oscillation. Also, in order to improve the signal-to-noise ratio, the RC charging time constants were reduced to 0.2 microseconds for both integration and second differentiation. The resulting fast pulses reach a peak before the single channel analyzer in Fig. 6 can generate a logic pulse. Therefore activation of the stretcher gate was changed to either the internal discriminators in the stretchers or a single external discriminator (not shown in Fig. 6) following amplifier 5. The system pulse shapes while using an 0.2 microsecond time constant are shown in Fig. 8.

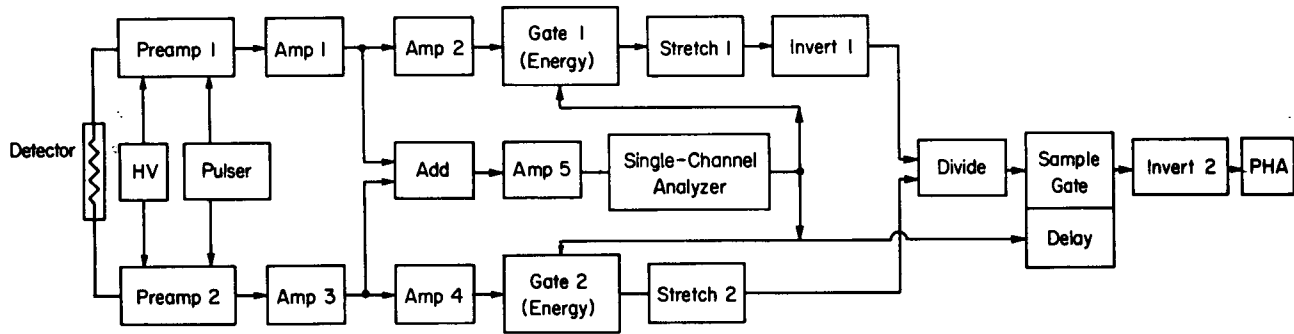


Figure 6 BLOCK DIAGRAM OF ELECTRONIC SYSTEM

Amp 1 Output
Amp 5 Output
SCA Output
Amp 2 Output
Gate 1 Open
Stretch 1 Output
Divider Output

Sample Gate Open
Sample Gate Output

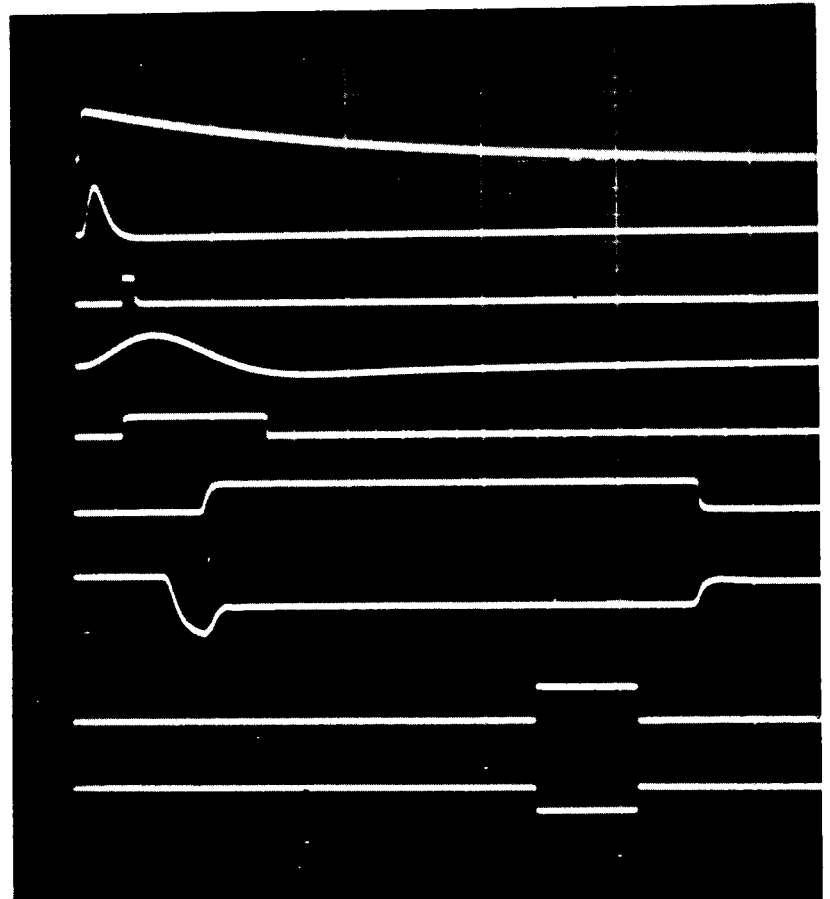


Figure 7 PHOTOGRAPH OF ACTUAL PULSES IN THE SYSTEM SHOWN IN FIG. 6 Sweep speed is 5 μ s/div.

Preamp 1 Output
Amp 2 Output
Gate 1 Open
Stretch 1 Output
Divider Output
Amp 5 Output
SCA Output
Sample Gate Open
Sample Gate Output

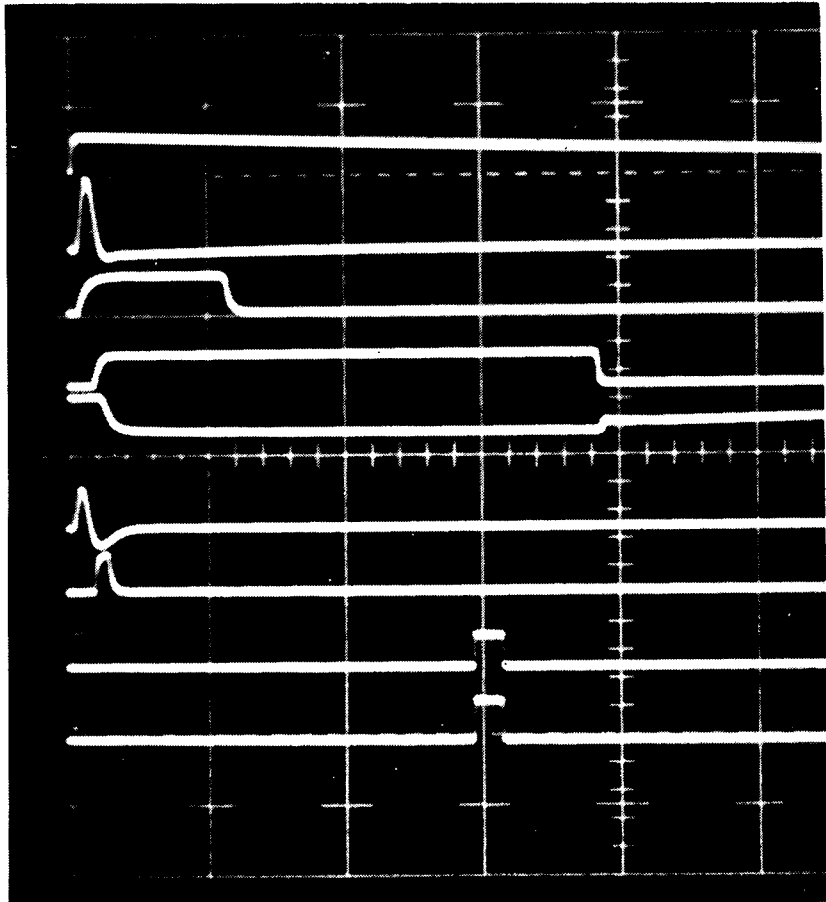


Figure 8 PHOTOGRAPH OF ACTUAL PULSES AFTER REDUCING AMP 2 TIMECONSTANT TO 0.2 MICROSECOND. Sweep speed is 5 μ s/div.

Table 3

NIM COMPONENTS USED FOR CIRCUIT SHOWN IN FIGURE 6

<u>Function</u>	<u>Component</u>
Preamp 1	Mechtronics 402
Preamp 2	Mechtronics 402
Amp 1, Amp 2	Tennelec TC-200
Amp 3, Amp 4	Tennelec TC-200
Energy Gate 1, Stretch 1	Ortec 442
Energy Gate 2, Stretch 2	Ortec 442
Invert 1	Tennelec TC-212
Divider	Burr-Brown 4098/25
Delay, Sample Gate	Tennelec TC-304
Invert 2	Ortec 433
PHA	Nuclear Data 130
Add	Ortec 433
Amp 5	Ortec 410
Single-Channel Analyzer	Ortec 420
HV	Mechtronics 253
Pulser	Tennelec TC-812

5. EXPERIMENTAL RESULTS: QUARTZ DIFFRACTION WITH
THE 137° COUNTER

The curved detector was mounted on a conventional GE powder camera for the diffraction tests. Pulverized Ottawa sand (74 micron) in an 0.3 mm capillary was used for the tests. Other data are in Table 4. These tests were somewhat abbreviated because of concurrent analyzer failures but are adequate to indicate the spectra obtainable.

Two samples of the quartz spectra are shown in Figs. 9 and 10. The spectra are similar except one was taken with a narrower window to improve the resolution by reducing the umbrella effect. No Soller slits are used. Generally good results were obtained over the full range of the spectra. Even with a non-uniform 5 mil anode, the resolution of the group around the 212 line indicates a system resolution of about 0.5 mm (0.4°) is being achieved. The peaks in the region from 201 to 110 happen to fall on a region of the wire with abnormally high gas gain and poor energy resolution. This caused some detection problems (see next section) and reduction in peak amplitude such as in Fig. 10.

Both Figs. 9 and 10 contain 2800 channels of data. The number of channels in one peak, say, the 211 peak, is about 20. This could be cut in half and still maintain good peak definition. The continuous line is a smoothed curve calculated using a 5 point quadratic smoothing formula.

An enlarged portion of the long counter spectrum in the vicinity of the 212 group is shown in Fig. 11 and compared with previous results using the short counter. The results indicate that a long counter system can be made with essentially the same resolution achieved with the earlier short counter. A more complete interpretation is that the new electronic system for

Table 4

EXPERIMENTAL CONDITIONS FOR FIGS. 9 AND 10

Geometry:	GE XRD powder camera with position sensitive counter mounted instead of film. Anode wire radius is 7.14 cm (2-13/16 in.). Dispersion is 8°/cm
Sample:	Pulverized Ottawa sand (< 74 micron)
Sample holder:	0.3 mm capillary
Sample rotation:	1 rpm
Collimation:	0.4 x 2.5 mm slit
X-ray tube:	CA-7H with chromium target, vanadic acid filter
X-ray tube voltage:	35,000 V
X-ray tube current:	1 ma
Exposure time:	20 minutes

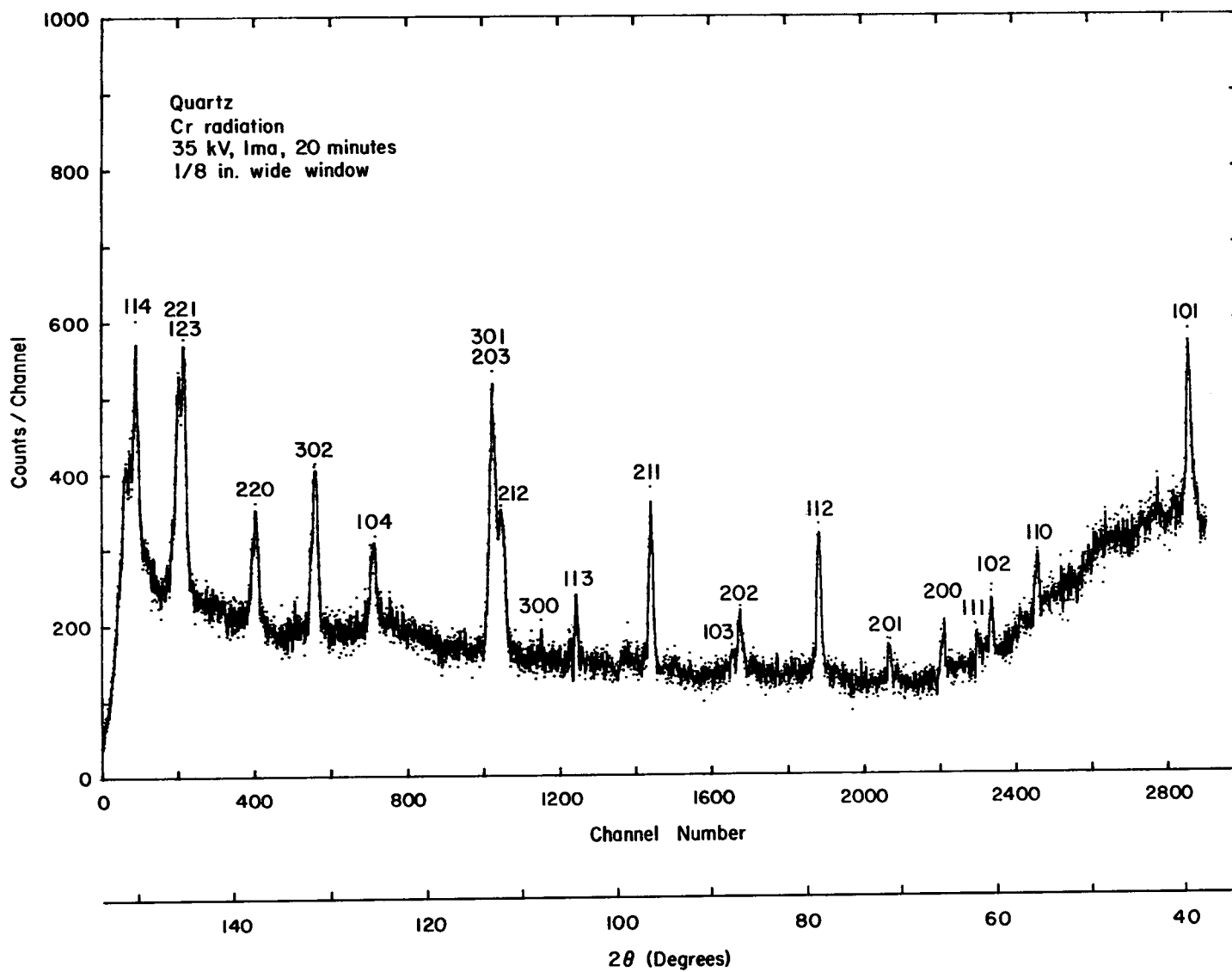


Figure 9 QUARTZ X-RAY DIFFRACTION SPECTRUM TAKEN WITH THE 137° COUNTER. Window width is 1/8 in. (3.2 mm).

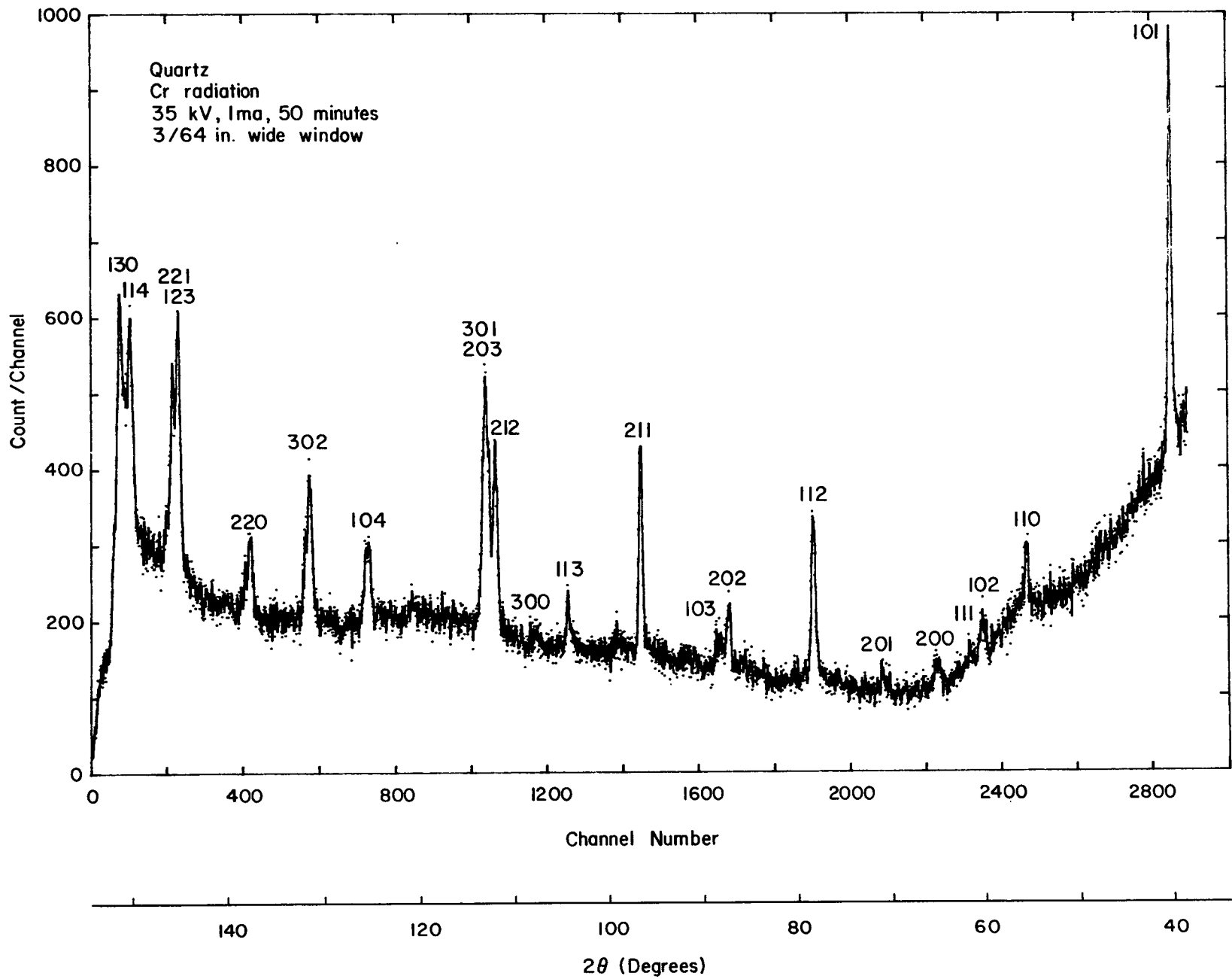


Figure 10 QUARTZ X-RAY DIFFRACTION SPECTRUM TAKEN WITH THE 137° COUNTER. Window width is 3/64 in. (1.2 mm).

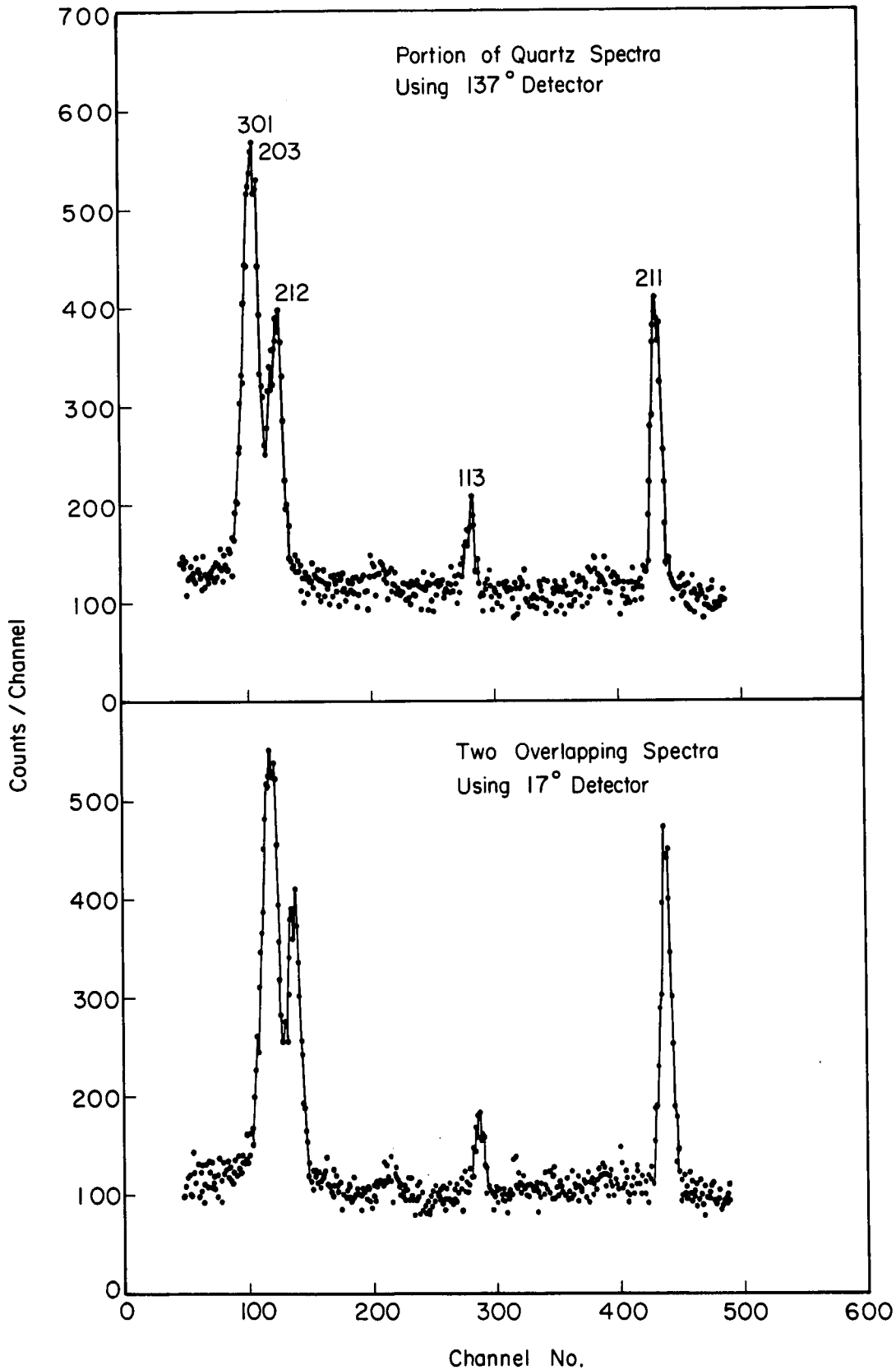


Figure 11 COMPARISON OF QUARTZ DIFFRACTION SPECTRUM TAKEN WITH THE 137° COUNTER AND THE 17° COUNTER. Exposure for the top (new) spectrum is 20 minutes at 35 kV and 1 ma. Exposure for each segment of the bottom (old) spectrum is 10 minutes at 35 kV and 25 ma.

the long counter compensates for the losses introduced by using a longer wire, i.e., the old short counter would give even better results if it were used with the new electronic system.

5.1 Energy Resolution

The primary problems encountered during the tests were associated with the non-uniformity of the anode. Significant variations (up to almost a factor of 2) in gas gain were observed along the wire as well as double peaks. A narrow energy-window therefore could not be used. There are two primary consequences of operating with a non-uniform wire: (1) the signal-to-noise ratio deteriorates because of the wide energy window required and (2) the position resolution deteriorates because the divider accuracy is significantly poorer for the small pulses generated at some portions of the wire. The overall spectrum quality therefore suffers although the basic operation as a position sensitive detector is not affected. An attempt was made to maintain at least a crude energy window but in practice the window was little more than a low level noise discriminator.

5.2 Sensitivity

Apart from the greater angular range, one other parameter is seemingly different for the new counter — the exposure. As is obvious in Fig. 11, the accumulated spectra are similar but the exposure required during tests with the short 17° detector last year is 250 ma-minutes whereas the exposure for the new 137° detector is 20 ma-minutes. There is nothing about the construction of the counters to cause such a difference. A qualitative side-by-side test of the old counter and the new counter indicated nearly equal sensitivity (the line intensity ratio was about 1.5). The most likely explanation for the present lower beam intensity is that the collimator alignment with the X-ray tube target is better now than during experiments last year with the old detector.

6. ANCILLARY STUDIES

6.1 Slant Path Effects

One of the important differences between a powder camera and a focusing camera is the angle between the diffracted X-ray beam and the detector. In a powder camera, the beam is perpendicular to the detector; in a focusing camera, the beam is at some angle to the detector causing a slant path through the detector. The effect of this slant path on resolution is analyzed in this section.

An X-ray beam generates free electrons all along its path through a detector. For most gases and X-ray energies ($E < 25$ keV) the electrons have a path length that is very short compared to the mean free path of the X-rays so the electrons remain in the vicinity of the X-ray beam. The exact amount of charge depends on the gas, but in all cases, the charge decreases along the path according to the exponential attenuation law. The free electrons produced by the X-ray along the path move in a straight line from the spot of creation to the anode wire. If the beam is perpendicular to the wire, all the charge is collected at one point. If the beam passes through the counter on a slant path, the charge will be collected over a wider region. The actual width of the collected charge distribution will depend on several factors such as gas composition, gas pressure, X-ray energy, and angle of incidence.

A rough measure of the significance of a slant path on line width can be obtained from the photon mean free path (mfp) since most (85 percent) of the charge is generated within a distance of 2 mean free paths. For Mn K_{α} X-rays in argon gas at 1 atmosphere pressure, the mfp is 19.7 mm. For xenon gas at 2 atmosphere pressure, the mfp is 2.3 mm. Significant effects can therefore be expected in both cases — particularly with argon.

Figure 12 is a schematic illustration of a photon beam passing through a counter. The intensity of the beam along the track is given by

$$I = I_0 e^{-\mu \rho t} \quad (1)$$

where I_0 is the intensity at the window, μ is the mass absorption coefficient, and t is the distance along the track. The distance, x , along the wire is related to t by $x = t \cos \theta$. If the charge produced within an element dt at t is ultimately collected and displayed as an apparent gaussian distribution centered at x , then the expected distribution, $Q(x)$, for an arbitrary slant path is given by

$$Q(x) = \frac{\mu \rho I_0}{\cos \theta W \sqrt{\pi}} \int e^{-\left(\frac{\mu \rho \xi}{\cos \theta}\right)} e^{-\left(\frac{\xi - x}{W}\right)^2} d\xi \quad (2)$$

where W is the width (half width at $1/e$) of the gaussian smearing function and ξ is a dummy position variable. The apparent smearing of even a highly collimated source is caused by (1) electronic noise, and (2) finite photoelectron range in the gas. Integration of Eq. (2) results in

$$Q(x) = \frac{\mu \rho}{2 \cos \theta} e^{-\frac{\mu \rho x}{\cos \theta}} \cdot e^{\left(\frac{\mu \rho W}{2 \cos \theta}\right)^2} \cdot \left[\operatorname{erf}\left(\frac{L}{W} - \frac{x}{W} + \frac{\mu \rho W}{2 \cos \theta}\right) - \operatorname{erf}\left(-\frac{x}{W} + \frac{\mu \rho W}{2 \cos \theta}\right) \right] \quad (3)$$

where $\operatorname{erf}(Z)$ is the error function defined in the usual way.

Figures 13 through 16 show a series of calculations made with various angles, gases, and pressures. The computer program used to generate these curves using Eq. (3) is listed in Appendix B as the program PROFILE. For these plots, a finite beam width of 0.22 mm was also assumed and included in the smearing function to match typical experimental conditions. The distance scale is the same within each figure. The scale for

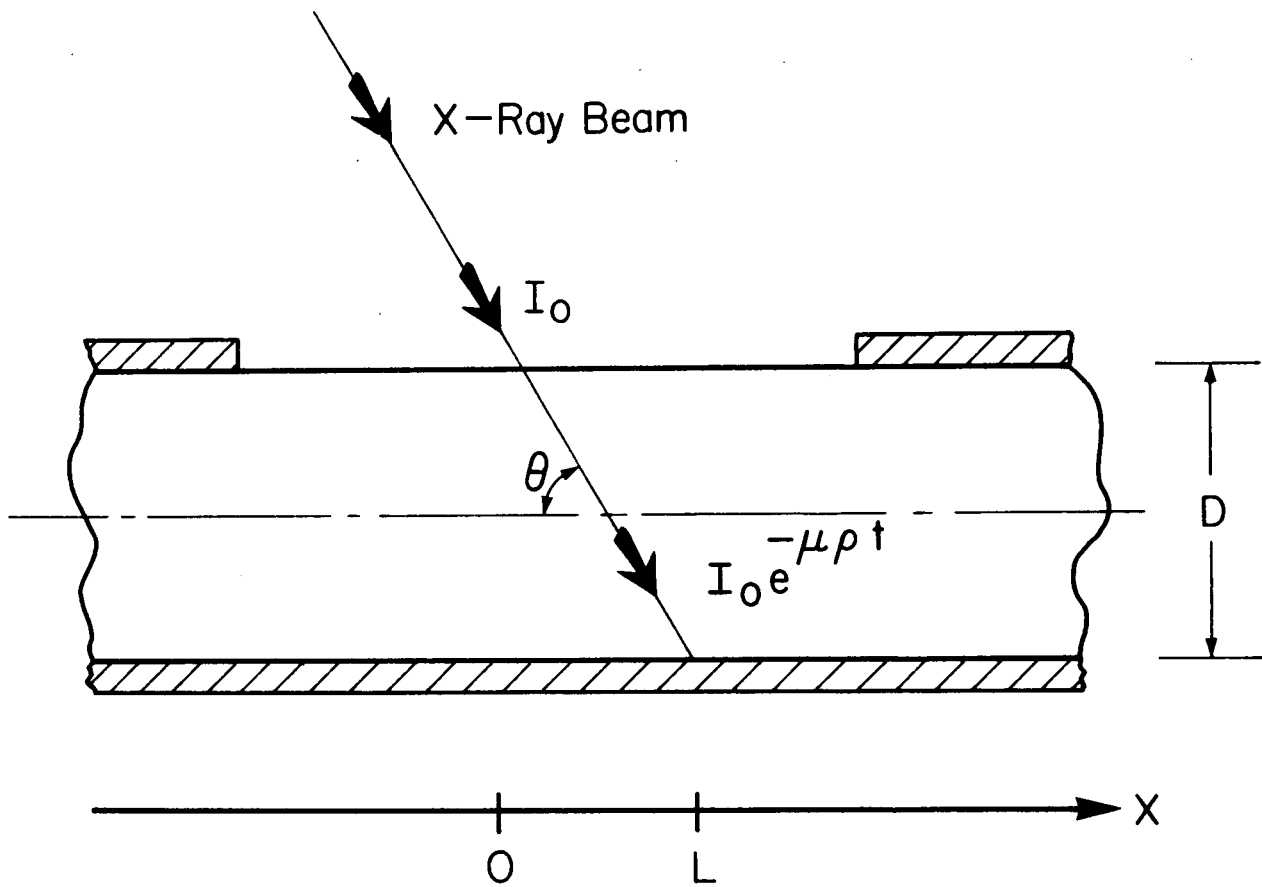


Figure 12 SCHEMATIC DIAGRAM SHOWING PARAMETERS USED TO DESCRIBE AN X-RAY BEAM PASSING THROUGH A DETECTOR ON A SLANT PATH

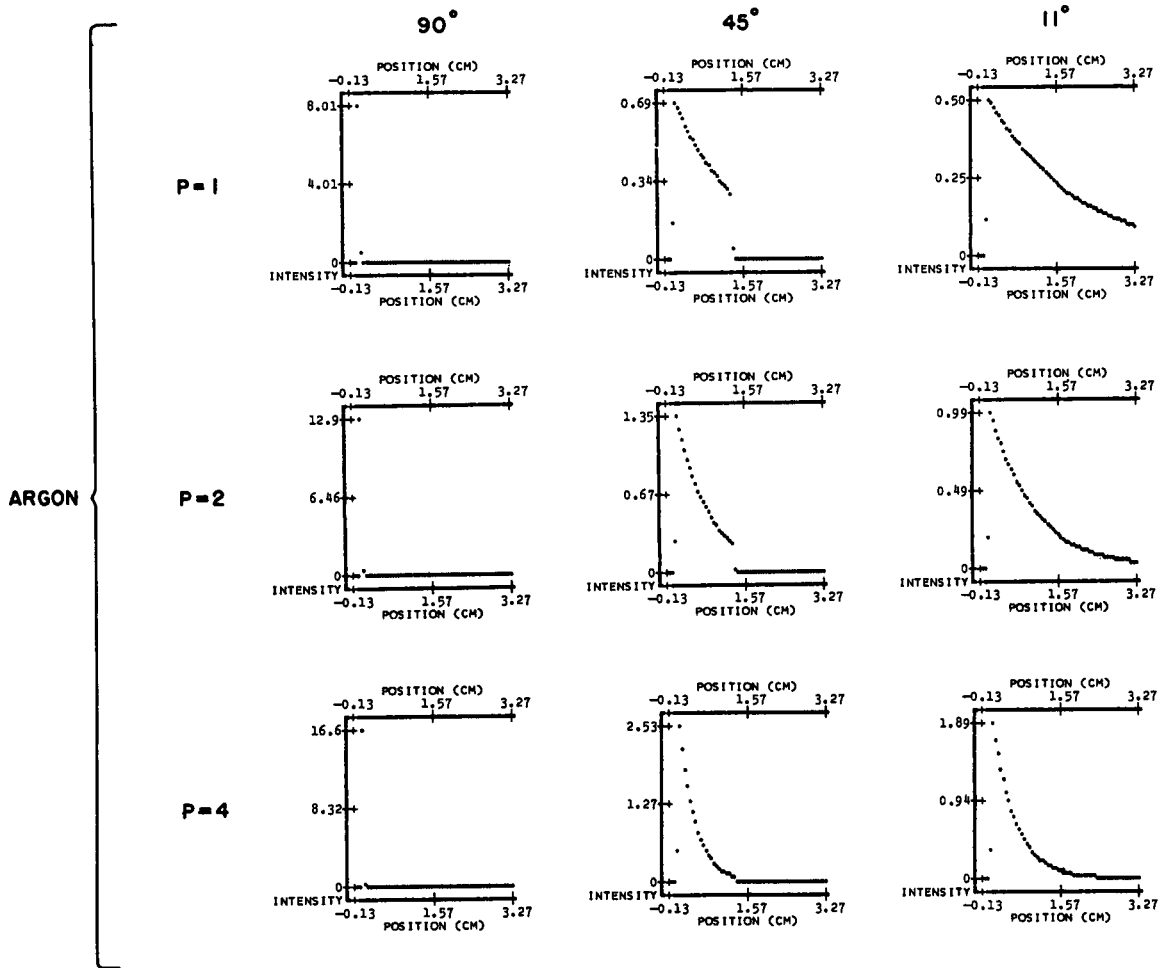


Figure 13 CALCULATED DETECTION PROFILES FOR SLANTPATHS IN ARGON PLOTTED ON A LARGE SCALE. Angles given at top are between the incident ray and anode wire; pressures are in atmospheres. The actual width of the incident beam is assumed to be 0.22 mm. Electronic noise equivalent to 0.25 mm is included.

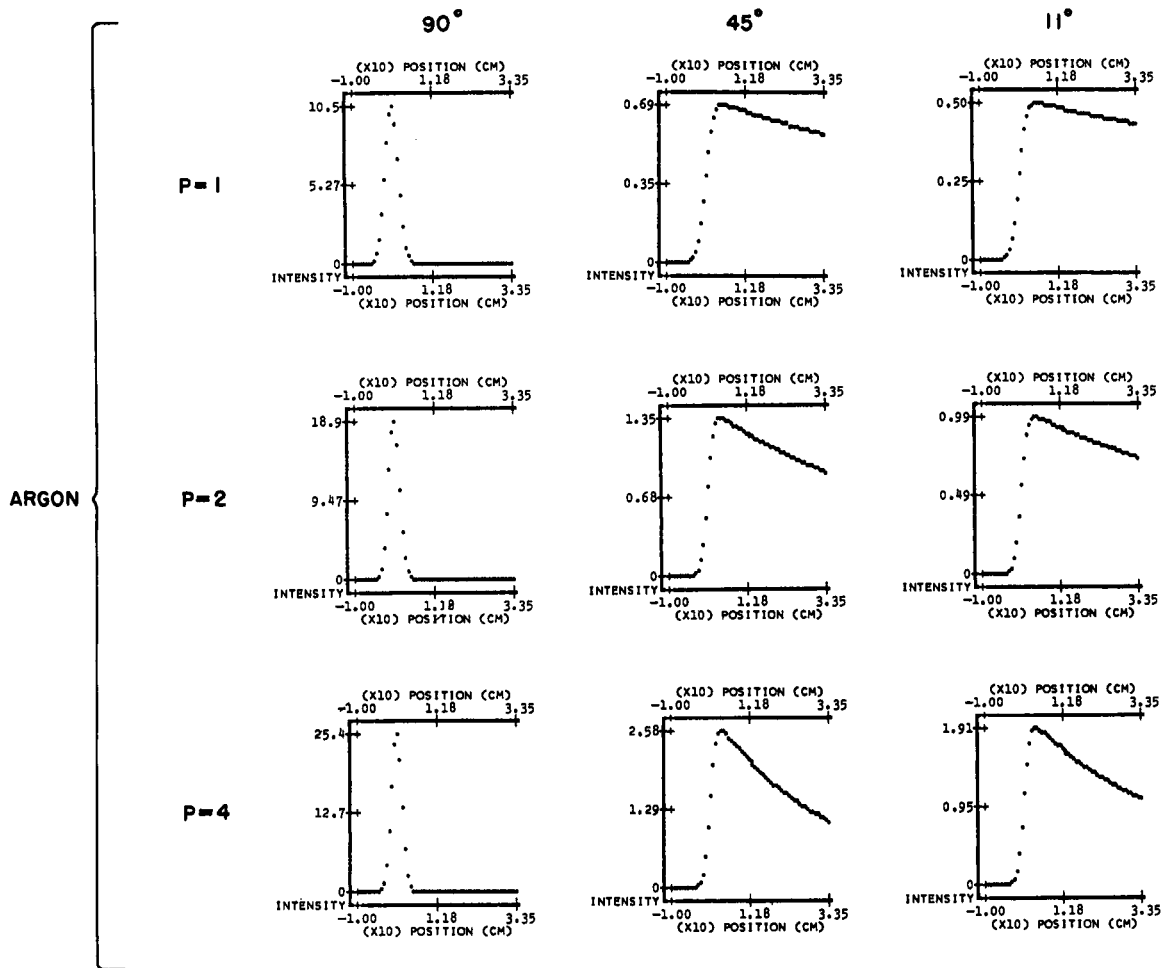


Figure 14 CALCULATED DETECTION PROFILES FOR SLANTPATHS IN ARGON PLOTTED ON A SMALL SCALE. Angles given at the top are between the incident ray and anode wire; pressures are in atmospheres. The actual width of the incident beam is assumed to be 0.22 mm. Electronic noise equivalent to 0.25 mm is included.

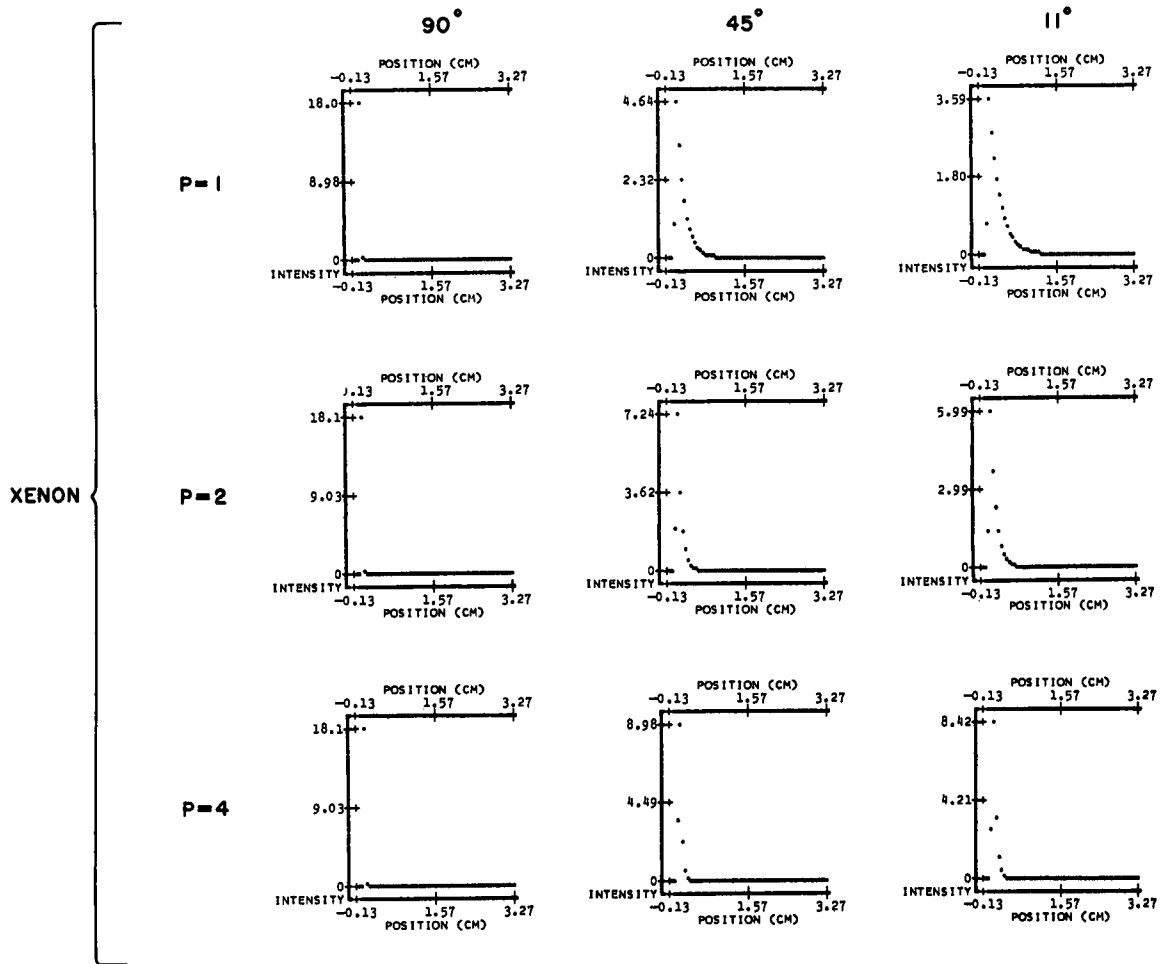


Figure 15 CALCULATED DETECTION PROFILES FOR SLANTPATHS IN XENON PLOTTED ON A LARGE SCALE. Angles given at the top are between the incident ray and the anode wire; pressures are in atmospheres. The actual width of the incident beam is assumed to be 0.22 mm. Electronic noise equivalent to 0.25 mm is included.

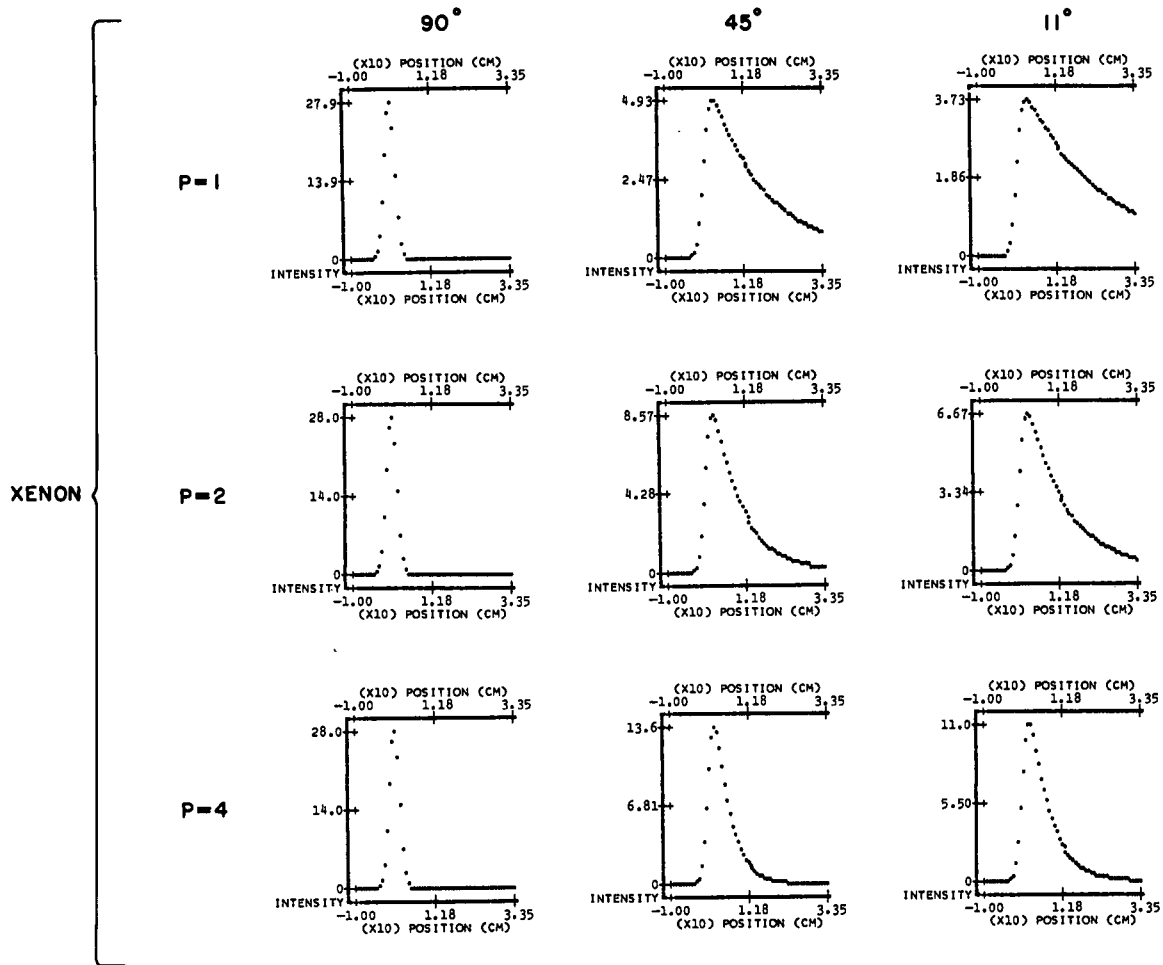


Figure 16 CALCULATED DETECTION PROFILES FOR SLANTPATHS IN XENON PLOTTED ON A SMALL SCALE. Angles given at the top are between the incident ray and anode wire; pressures are in atmospheres. The actual width of the incident beam is assumed to be 0.22 mm. Electronic noise equivalent to 0.25 mm is included.

Figs. 13 and 15 are relatively large and shows the gross effects. The scale in Figs. 14 and 16 was picked to show more detail in the line shapes.

Experimental verification of these results was obtained for a slant path at 65.7° in 1 atmosphere of argon. Figure 17 shows the observed charge distribution and the theoretical distribution calculated for the same number of interactions. The distribution extends from wall to wall in the detector. The general agreement is good. The scatter in the data is caused by the relatively small number of collected counts. The count rate was low (< 2 counts/min) because of collimation, even though a helium filled tunnel was used along part of the path to minimize attenuation losses. The data is not smoothed.

In order to minimize the loss of resolution from slant paths, the use of a heavy gas, such as xenon, at elevated pressure is indicated. A significant increase in voltage is required on both counts. The approximate operating conditions for a somewhat smaller diameter detector can be estimated as follows:

The gas multiplication (M) is functionally related to the voltage (V), pressure (p), wire radius (r), and cylinder radius (R) by

$$\ln M = f\left(\frac{V}{\ln\left(\frac{R}{r}\right)}, rp\right) \quad (4)$$

For a 2.5 mil anode, a decrease in R from the present 0.25 in. to 0.125 in. will decrease $\ln\left(\frac{R}{r}\right)$ from 4.6 to 3.9. A corresponding decrease in voltage to 1700 V would maintain the same gas multiplication. For an argon filled counter with R = 0.125 in., r = 0.0025 in., and V = 1700, the Diethorn⁽³⁾ equation indicates that pressures of 1, 2, 3, and 4 atmospheres requires 1700 V, 2600 V, 3400 V, and 4200 V, respectively, to maintain the same gas gain. Since xenon operating voltages are typically 20 percent higher than those for argon, xenon at 1, 2, 3, and 4 atmospheres pressure

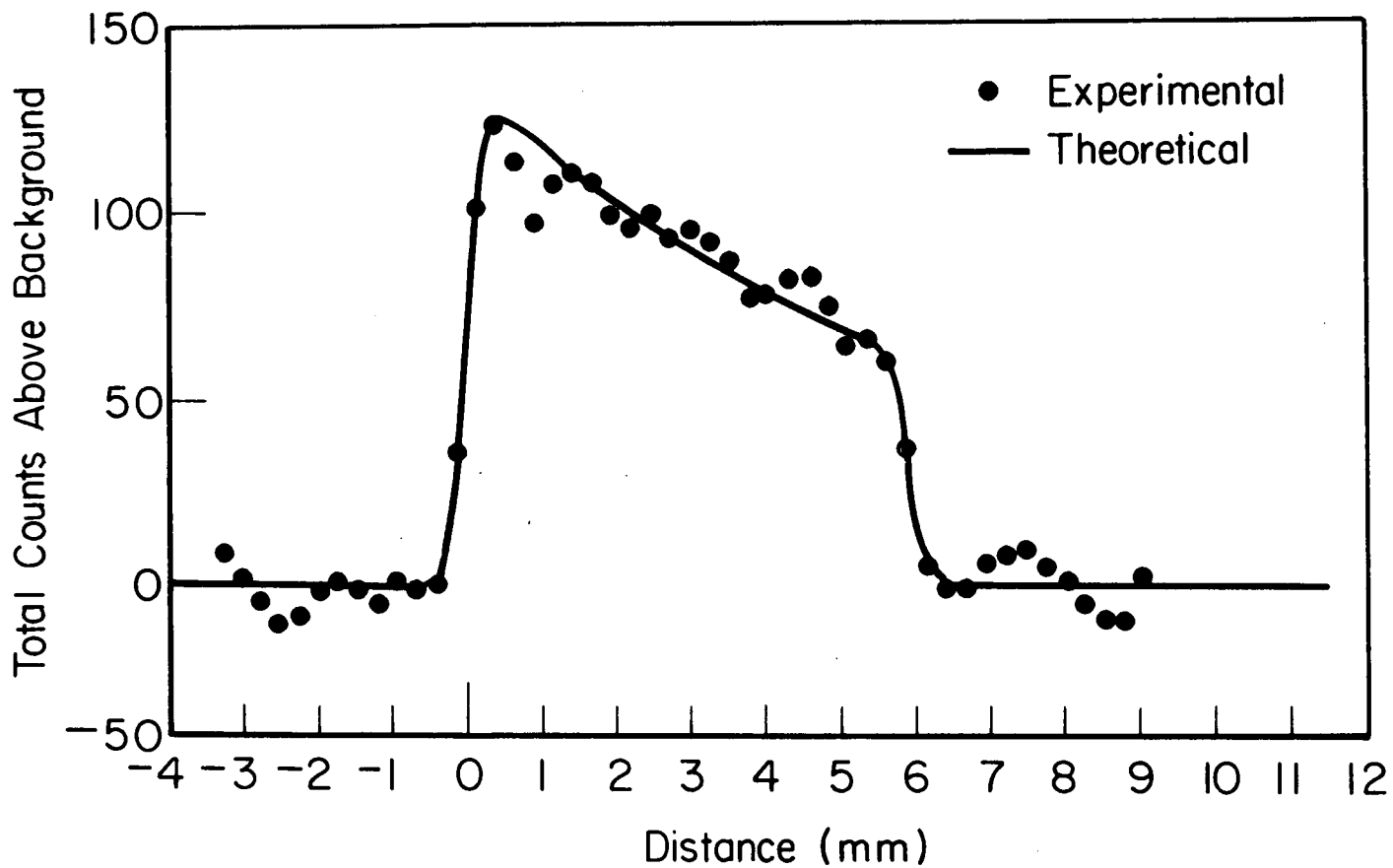


Figure 17 COMPARISON OF THE OBSERVED AND CALCULATED CHARGE DISTRIBUTION AT THE ANODE WIRE FROM AN X-RAY BEAM AT AN ANGLE OF 67.5° . The calculated curve is for the same total number of interactions (same area) as the experimental data.

would require about 2040 V, 3120 V, 4080 V, and 5040 V, respectively. However, in a 1/4-in. diameter counter, 3000 volts is about the maximum tolerable voltage because of breakdown problems. A small counter therefore will be limited to about 2 atmospheres of xenon. The resolution would then vary from 0.3 mm when the path is perpendicular to the wire to about 1.1 mm when the path makes an 11° angle with the wire.

6.2 Anode Support Systems

Although the present counter has been successfully operated with a free-standing anode, the question of supports and their effect on the spectra is an important one. Several different support geometries were tested for their effect on the position spectrum. These are schematically illustrated in Fig. 18 and briefly described in Table 5. Typical supports near a 1 mil anode disturb the electric field for a total distance of 1 to 2 cm. The minimum disturbance appears to be about 0.6 cm for the systems tested. The scheme shown as 3b has not been tested.

The various geometries were constructed in a versatile straight test counter which permits an easy interchange between 3 different cathodes, 4 different anode supports, and 3 different anode wires. Both metal and plastic posts were included because of inconclusive results from another counter which seemed to indicate less disturbance from a metal post. The present results indicate approximately equal effects from a metal post and plastic post. Although not measured, a visual estimate of energy resolution indicated better resolution with the plastic post. This is probably because the wall is relatively undisturbed when using a plastic post but a large hole in the counter wall is required for insulation of the metal post.

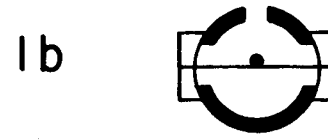
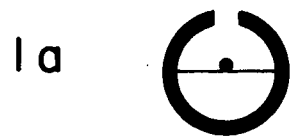


Figure 18 SCHEMATIC CROSS SECTIONAL VIEW OF ANODE SUPPORT SCHEMES. Dark regions are conductive; open regions are insulators.

Table 5
SUPPORT GEOMETRIES AND THEIR EFFECT ON THE POSITION
SPECTRUM WHEN USING 1 MIL ANODE

<u>Description</u>	<u>Closest Figure</u>	<u>Approximate Region Affected (cm)</u>
(1) Transverse 5 mil glass fiber, metal wall	1a	1.2
(2) Transverse 5 mil nylon fiber, metal wall	1a	1.5
(3) Transverse 0.7 mil nylon fiber, metal wall	1a	1.0
(4) Transverse 4 mil ss wire, insulated wall	1b	2.4
(5) Transverse 5 mil carbon-on-quartz, insulated wall	1b	2.3
(6) Nylon post, 4 mil ss loop metal wall	2a	2.0
(7) Nylon post 1.5 mm short, 0.7 mil nylon loop, metal wall	2a	0.6
(8) Nylon post, 5 mil nylon loop, metal wall	2a	1.6
(9) Metal post, 4 mil ss loop, insulated wall	2b	2.7
(10) Metal post, 1.5 mil nylon loop, insulated wall	2b	1.4
(11) 5 mil plastic loop, metal wall	3a	1.8
(12) 15 mil glass post, 1 mm gap; metal wall	2a without loop	0.6
(13) 16 mil metal post, 1 mm gap; insulated wall	2b without loop	0.9
(14) 15 mil glass post touching anode; metal wall	2a without loop	2.0
(15) 16 mil metal post touching anode; insulated wall	2b without loop	1.8

Generally one finds that a heavy support post can extend to within a millimeter or two of the anode wire with very small effects on gas amplification. The part that actually touches the wire should be as small as possible, however. The best support system examined consisted of a nylon post extending to within 1.5 mm and then an 0.7 mil nylon loop around the anode. A finger of 0.7 mil nylon attached to the anode with epoxy would probably be better yet. Dr. S. I. Baker, at this laboratory, has successfully attached 1 mil support fibers to 5 mil anode fibers using a butt-joint with barely perceptible epoxy.

6.3 Pure Carbon Anodes

In addition to the quartz fibers coated with pyrolytic carbon, test samples of pure carbon fibers have also been obtained for use as anode "wires." Dr. J. Spijkerman of the National Bureau of Standards originally suggested carbon as a substitute. Although the results were not quite as good as those obtained with the quartz fibers, the material is usable if rigidity is not required.

Commercial grade carbon yarn⁽⁴⁾ was purchased for the test. The yarn is available both as graphite and pyrolytic carbon. Only the carbon material has been tested. The yarn consists of 2400 monofilaments with a diameter of about 0.4 mil. Individual filaments about 6 inches long were removed without difficulty. The individual fibers appear to contain score marks similar to those observed on metal wire. Presumably these marks are retained from the plastic fiber used as raw material for the yarn. The resistance is approximately 19,000 ohms per inch.

Figure 19 is a position spectrum of a double slit obtained with this material. The FWHM of the peaks is approximately 0.7 mm compared to a result of about 0.4 mm using the coated fiber. This measurement was made in the test bed using an 0.56 in. diameter

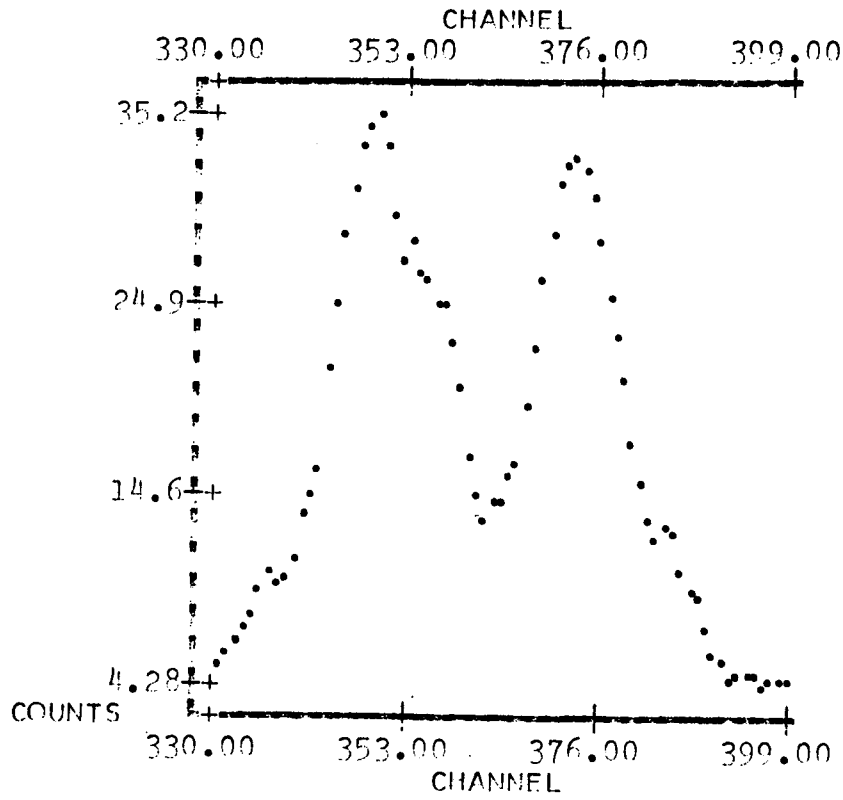


Figure 19 RESPONSE OF AN 0.4 MIL PURE CARBON ANODE USING A DOUBLE SLIT COLLIMATOR. FWHM of the peaks is about 0.7 mm. Eleven point quadratic smoothing has been used.

counter operated at 1180 volts with P-10 gas. No effort was made to improve or optimize the response. Possibly a higher voltage would yield results comparable to those obtained with the coated fiber material.

6.4 Resolution Limitations

The primary factor which presently limits the position resolution is preamplifier noise. The initial expectation was that replacement of the hard-tube preamplifiers with solid state preamplifiers would significantly reduce the noise levels and improve the position resolution. While an improvement was achieved, the effect was minimal. Since the cause and cure of the system noise level was not as clear as supposed earlier, this point has been examined in more detail.

The observed characteristics of the short counter (used with hard-tube preamplifiers) and the 137° counter (used with solid state preamplifiers) are tabulated in Table 6.

To help sort out the importance of wire resistance, preamplifier characteristics, and other factors affecting resolution, the early system was reconstructed and slowly converted to the present system while the system parameters were monitored.

Starting with approximately the original hard-tube electronic system (several components are no longer available), and the original short-arc counter, the first component changed was the preamplifiers. No improvement in resolution was noted as a result of switching from hard-tube to FET input preamplifiers (pulser FWHM = 7.7 and 7.9 channels, respectively).

The time constant was then decreased from 12.8 to 1.6 μ s. The analog divider output never actually stabilizes with this fast pulse but it was usable with a short (1.4 μ s) sampling gate located at the point with minimum slope. The pulser resolution

Table 6

TABULATION OF PARAMETERS RELATED TO POSITION
RESOLUTION FOR THE SMALL AND LARGE COUNTER

	<u>Short 15° Counter</u>	<u>Long 137° Counter</u>
Resolution (overall)	0.4 mm	0.4 mm
Noise contribution to resolution (pulser width)	0.13 mm	0.25 mm
Slit width contribution to resolution	0.22 mm	0.22 mm
Inherent detector contribution to resolution (balance)	0.29 mm	0.28 mm
Preamplifiers	Hard-tube (Tennelec 100B)	Solid State (Mechtronics 402)
Shaping Time Constants	12.8 μ s	0.2 μ s
Anode Resistance	250 K ohms	75 K ohms
Anode Length	3.2 cm	18.1 cm

was improved the same amount with both the hard-tube and solid state preamplifiers (pulser FWHM = 3.0 and 3.1 channels, respectively).

Introduction of the pulse stretchers to provide stable signals into the divider resulted in a reduction of pulser widths to 2.4 and 2.3 channels with the hard-tube and solid state preamps.

A further decrease in the time constant to 0.2 μ s produced a further reduction in pulser widths to 1.6 and 1.4 channels for the hard-tube and solid state systems.

A total reduction in pulser width from 8 channels to 1.6 channels had been achieved previously with the original hard-tube system but only by increasing the tube voltage in order to increase the gas amplification. The use of short time constants and stretchers achieves the same result while leaving the high voltage at a better value for energy resolution. The solid state preamplifiers are not required to achieve this improvement in signal-to-noise ratio.

A switch from the short arc counter to the long arc counter (longer but with lower anode resistance) causes a small loss of resolution. The pulser widths after this change were 1.8 and 1.9 channels, respectively.

A significant contribution to this width is still caused by preamplifier noise. If the output from only one preamplifier is used to drive the system so that the noise on the two divider inputs is correlated, the pulser width drops from 1.9 to 1.3 channels with the solid state preamplifier.

When a single preamplifier is connected to the detector, the noise is a factor of 3 to 4 less than when both preamplifiers are connected. With a single preamplifier, the noise does not depend greatly on the resistance of the load; either one of the two detectors, no detector, or a pure 100 K ohm load can be applied with only a small change in noise level.

The lack of benefit from solid state preamplifiers in this system is apparently due primarily to the large input capacitance presented by the "other" preamplifier at the opposite end of the anode wire. The noise observed with a second preamplifier at the opposite end of the anode wire is essentially the same as when a dummy load of 100 K ohm and 20,000 pf capacitance (the approximate hot capacitance of the preamplifier) is applied.

6.5 0.1 Percent Analogue Divider Tests

The original module used for pulse division was the Burr-Brown 4098/25. A second divider with specifications indicating twice the speed and ten times the accuracy was also obtained (GPS 504). The primary specifications for these two modules are given in Table 7. In practice, the characteristics are quite different. The Burr-Brown will settle to the final value in 10-20 μ s, the GPS module requires about 30 μ s. The noise level as the output of both the Burr-Brown and GPS is 5 to 10 mv (PP).

Table 7
PRIMARY QUOTED CHARACTERISTICS OF THE
BURR-BROWN 4098/25 AND GPS 504

	<u>Burr-Brown 4098/25</u>	<u>GPS 504</u>
"Accuracy (% of FS)"	1 %	0.1 %
"Bandwidth (full scale)"	-	500 kHz
"Bandwidth (full power output)"	200 kHz	
"Output Drift"		0.5 mV/°C
"Output Offset vs Temp"	\pm 1 mV/°C	
"Scale Factor Drift"		0.02 %/°C
"Accuracy Drift"	\pm 0.05 %/°C	

The stability over a 200 minute period is approximately the same although the Burr-Brown unit is slightly better. The Burr-Brown also calculates $x/x+y$ whereas the GPS calculates only x/y . Accuracy, per se, was not specifically tested. Considering that the GPS unit costs about 5 times as much, the original Burr-Brown unit has proved to be a better unit on all counts – both performance and cost.

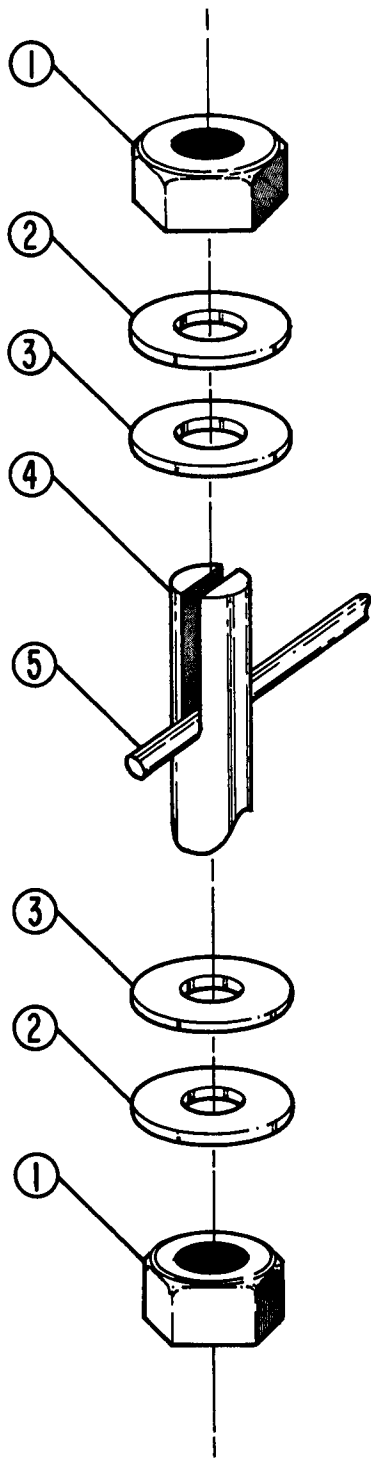
7. REFERENCES

- (1) R. A. Semmler, "Position-Sensitive X-Ray Detector for Diffraction Analysis," Final Report V1000, Internal Research and Development Project, IIT Research Institute, Chicago, Illinois (July 1968).
- (2) R. A. Semmler, "Testing of a Curved Position-Sensitive X-Ray Detector Using Diffracted X-Rays," Final Report V1037, Internal Research and Development Project Report, IIT Research Institute, Chicago, Illinois (April 1970).
- (3) R. A. Semmler, "A Curved Position-Sensitive Detector for X-Rays," pp. 399-408 in C. A. Ziegler, Ed., Applications of Low Energy X- and Gamma Rays (Gordon and Breach, London, 1971).
- (4) Robert W. Kiser, "Characteristic Parameters of Gas Tube Proportional Counters," Appl. Sci. Res. Section B, 8, 183-200 (1960).
- (5) Carborundum Co., Graphite Products Division, P.O. Box 577, Niagra Falls, New York, 14302, Grade GSCY 2-5 ply carbon.
- (6) Fibers generously provided by Mr. C. M. Zvanut, General Electric Co., Missile and Space Division, Spacecraft Dept., Valley Forge Space Technology Center, P. O. Box 8555, Philadelphia, Pa., 19101.

PRECEDING PAGE BLANK NOT FILMED

APPENDIX A

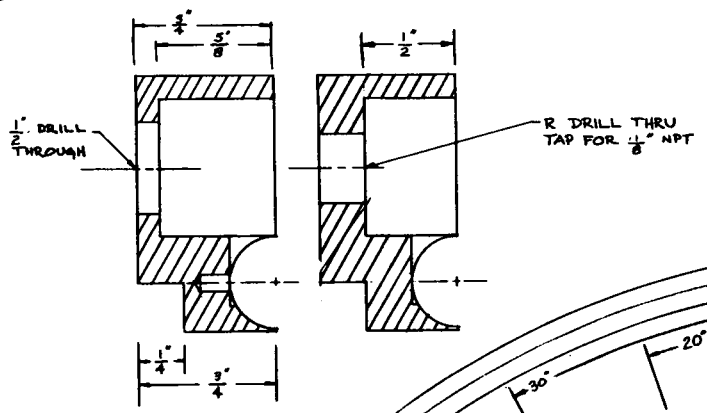
DRAWINGS FOR THE 137° COUNTER



- ① 2-56 NYLON NUT
- ② BRASS WASHER
- ③ CONDUCTIVE GASKET
- ④ SLOTTED NYLON 2-56 SCREW
- ⑤ ANODE WIRE

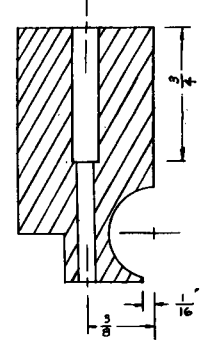
Figure A-1 ANODE WIRE SUPPORT SCHEME USED IN THE 137° COUNTER.

① SECTION THRU AA, PIECE 1 AND 2

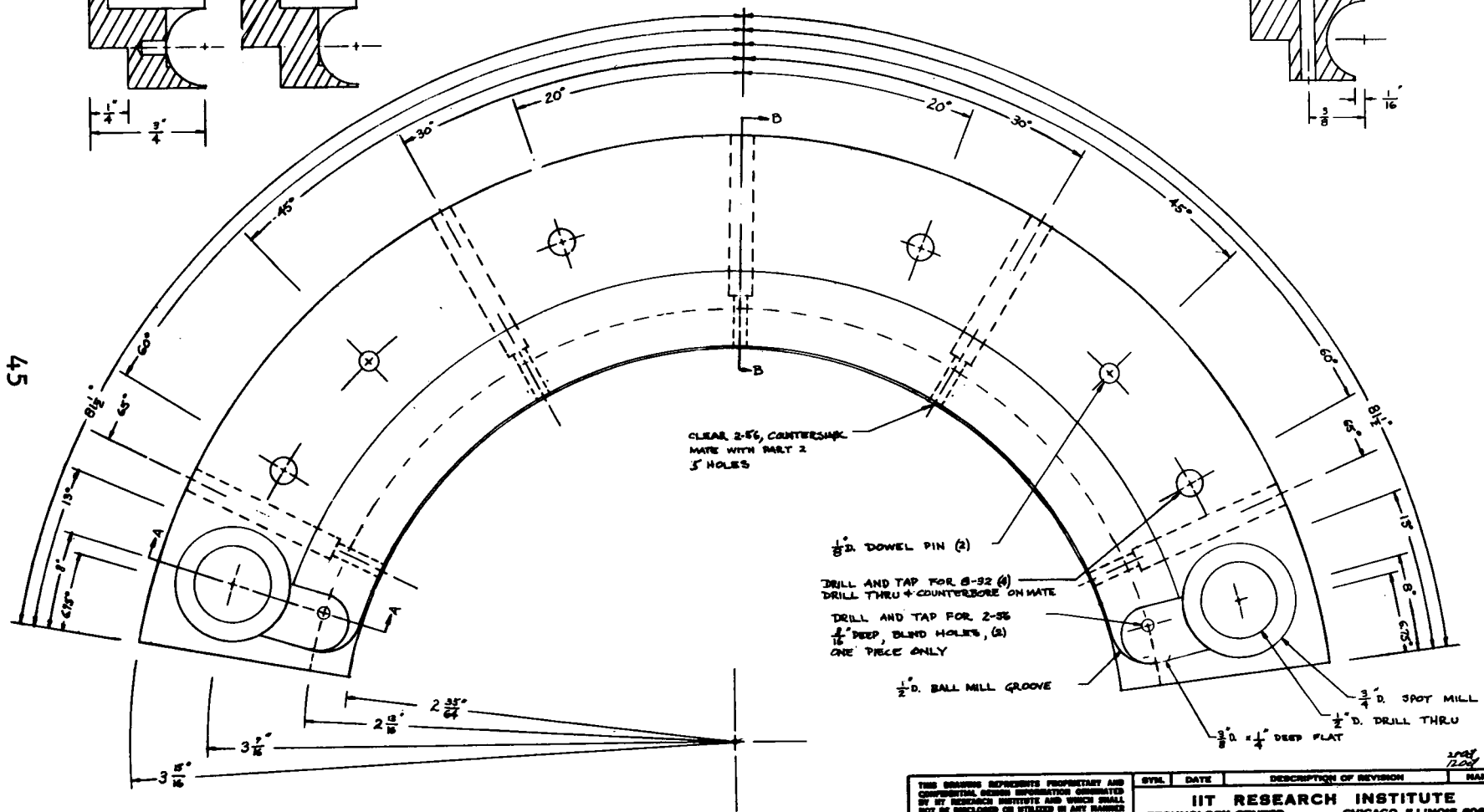


- NOTE: ① MAKE TWO, SAME EXCEPT DOWEL PINS AND 4-40 TAP.
 ② $2 \frac{15}{16}$ R. TO MATE WITH GF CAMERA

SECTION THRU B-B



47



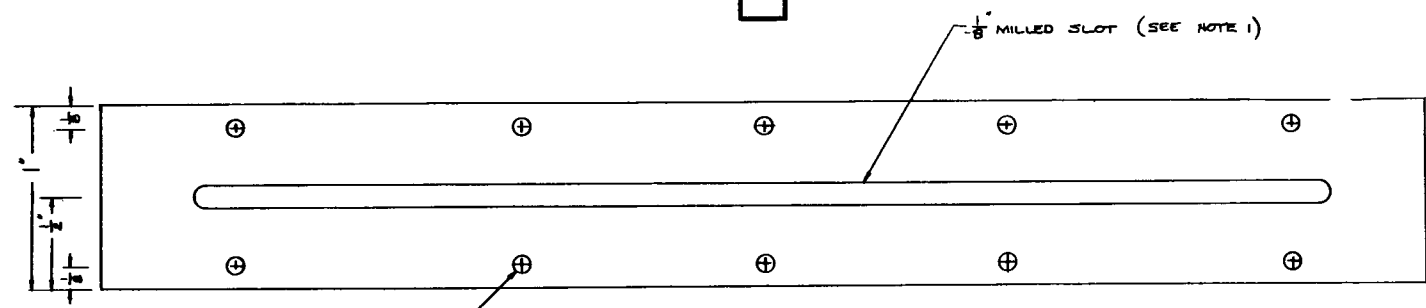
CLEAR 2-56, COUNTERSINK MATE WITH PART 2 3/4 HOLES

- 1/8" D. DOWEL PIN (2)
- DRILL AND TAP FOR 8-32 (4)
DRILL THRU + COUNTERBORE ON MATE
- DRILL AND TAP FOR 2-56
1/16" DEEP, BLIND HOLES, (2)
ONE PIECE ONLY
- 1/2" D. BALL MILL GROOVE
- 3/4" D. SPOT MILL
- 1/2" D. DRILL THRU
- 3/8" D. 1/4" DEEP FLAT

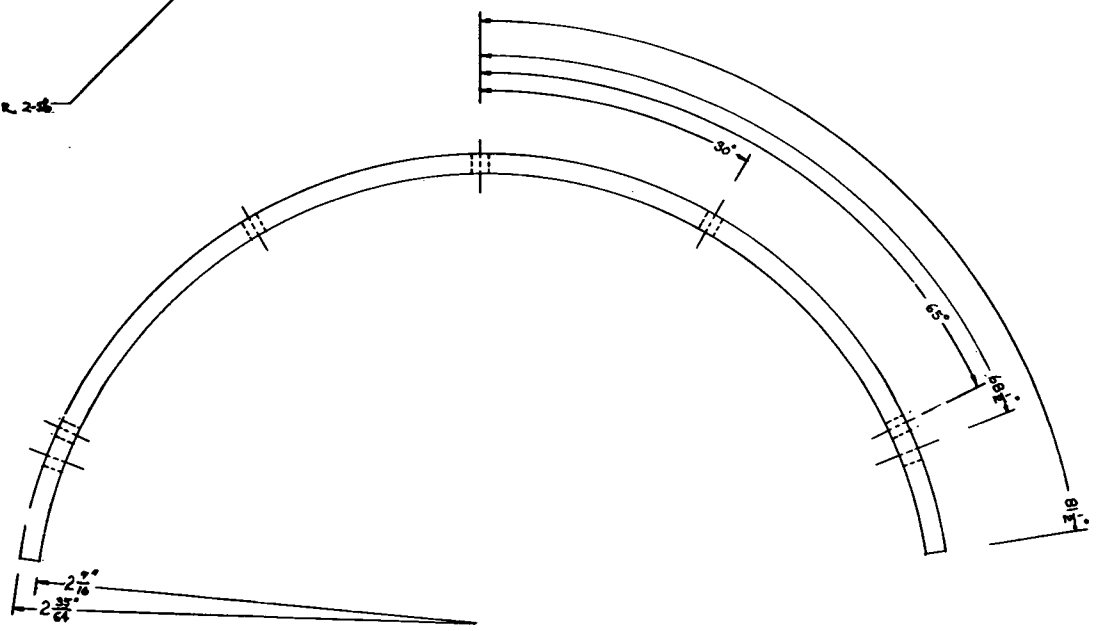
THIS DRAWING REMAINS PROPRIETARY AND CONFIDENTIAL UNLESS SEPARATION ORIGINATED BY IIT RESEARCH INSTITUTE AND WHICH SHALL NOT BE REPRODUCED OR UTILIZED IN ANY MANNER WITHOUT PROPER WRITTEN AUTHORIZATION.		SYBL	DATE	DESCRIPTION OF REVISION	NAME	
		IIT RESEARCH INSTITUTE TECHNOLOGY CENTER CHICAGO, ILLINOIS 60618				
MATERIAL BRASS HEAT TREAT		137° CURVED COUNTER				
TOLERANCES UNLESS OTHERWISE SPECIFIED FRACTIONS ± 1/64 DECIMALS ± .005 THIS CLASS ± .015 ANGULAR ± 1°		FINISH ✓	QUANTITY PER	DRAWN	CHECKED	APPROVED
DO NOT SCALE - REPORT ERRORS BREAK ALL SHARP CORNERS CHECK ALL TAPPED HOLES 1/32 ± .001 REMOVE BURRS			SUB-ASSEMBLY DATE 12-25-68	NAME DATE 12-23-68		
		SCALE	NEXT ASSEMBLY NO.	PROJECT DRAWING NO.		
		2x		-C-		

2

NOTE: ① MAKE 2, $\frac{1}{16}$ " MILLED SLOT IN SECOND PIECE
 ② MATE WITH PART 1
 ③ 1" WIDTH TO CLEAR SLOT IN GE CAMERA



DRILL AND TAP FOR 2-5/16
 10 HOLES



46

<small>THIS DRAWING REPRESENTS PROPRIETARY AND CONFIDENTIAL DESIGN INFORMATION ORIGINATED BY IIT RESEARCH INSTITUTE AND WHICH SHALL NOT BE DISCLOSED OR UTILIZED IN ANY MANNER WITHOUT PROPER WRITTEN AUTHORIZATION.</small>		SYNL	DATE	DESCRIPTION OF REVISION	NAME
IIT RESEARCH INSTITUTE TECHNOLOGY CENTER CHICAGO, ILLINOIS 60616					
MATERIAL BRASS		137° CURVED COUNTER			
HEAT TREAT		QUANTITY PER	DESIGNED	DRAWN	CHECKED
TOLERANCES <small>UNLESS OTHERWISE SPECIFIED FRACTIONS ± 1/64 DECIMALS ± .005 THIS CLASS ± .015 ANGULAR ± 1°</small>		<input checked="" type="checkbox"/>	DATE	DATE	DATE
<small>NO 90° SCALE - REPORT ERRORS BREAK ALL SHARP CORNERS CHISEL ALL TAPPED HOLES 1/32 ± .001 REMOVE BURRS</small>		SUB-ASSEMBLY SCALE	NEXT ASSEMBLY NO.	PROJECT DRAWING NO.	
		2x			-C-

2004 10
 120d'70

③ 2-56 x $\frac{19}{32}$ THREADED NYLON STOCK
WITH 0.01" SAW SLOT TO $\frac{1}{4}$ " DEPTH (2)

④ $\frac{3}{32}$ " ID x $\frac{3}{16}$ " OD. x 0.03" THICK WASHER,
USE 0.08" CONDUCTIVE GASKET STOCK (6)



-C-

Reproduced from
best available copy.

THIS DRAWING REPRESENTS PROPRIETARY AND CONFIDENTIAL DESIGN INFORMATION OBSERVED BY IIT RESEARCH INSTITUTE AND WHICH SHALL NOT BE DISCLOSED OR UTILIZED IN ANY MANNER WITHOUT PROPER WRITTEN AUTHORIZATION.		SYMBOL	DATE	DESCRIPTION OF REVISION	NAME
		IIT RESEARCH INSTITUTE TECHNOLOGY CENTER CHICAGO, ILLINOIS 60616			
MATERIAL		137° CURVED COUNTER			
HEAT TREAT					
TOLERANCES UNLESS OTHERWISE SPECIFIED FRACTIONS ± 1/64 DECIMALS ± .005 THIS CLASS ± .010 ANGULAR ± 1°		FINISH	QUANTITY PER	DESIGNED	DRAWN
DO NOT SCALE - REPORT ERRORS BREAK ALL SHARP CORNERS CHAMFER ALL TAPPED HOLES 1/32 x 45° REMOVE BURRS		✓	SCALE	DATE	CHECKED
UNLESS OTHERWISE NOTED			NEXT ASSEMBLY NO.	DATE	APPROVED
		PROJECT DRAWING NO.		-C-	

PRECEDING PAGE BLANK NOT FILMED

APPENDIX B

COMPUTER PROGRAM LISTINGS AND
SAMPLE EXECUTIONS

IIT RESEARCH INSTITUTE

APPENDIX B

Several conversational APL programs were written during the course of the program. These were used for both data reduction and calculation of theoretical results. The primary programs are tabulated below with a brief description. Program listings and sample executions are given on the succeeding pages. No other documentation is available. (Minor differences may be noted between the listing and execution since they were prepared at different times.)

1. INPUT - Provides keyboard entry of data with convenient means for entering corrections.
2. SMOOTH - Smooths or differentiates data using a piecewise least-squares polynomial. The degree of the polynomial and the number of points fitted is arbitrary.
3. GFIT - Computes position, width, and intensity of an arbitrary number of gaussian peaks sitting on an arbitrary degree polynomial background. Poisson weights may be included if desired. Variance is calculated. A straightforward normal equation solution is used which limits the number of peaks to two or three.
4. PROFILE - Computes the charge distribution at the anode (line profile) for an X-ray beam entering the counter on a slant path (see Eq. 3). Gas composition can be any of the usual counting gases. Gas pressure, and entry angle are arbitrary.

The first report on this project described APL as an extraordinarily versatile language which permits an easy implementation of complex calculations. This view has not diminished during the course of the program.

```

VINPUT [ ]V
V INPUT;ANS;CHAN;CORR;DATA;ENTRY;EVEN;FIRST;HIROW;INDEX;LAST;LIST;LOROW;M;NEW;NO;OBLIT;PAD;
  PADDED;ROWS;SAME;TYPE;YES
[1]  A THIS PROGRAM ACCEPTS PHA DATA AND ANY CORRECTIONS.
[2]  A DATA IS STORED AS VECTOR Y.
[3]  A REQUIRES CSTN, CSTV, DFT, AND Y.
[4]  A ENTER DATA
[5]  INIT+ ' ' CSTV 38+ ,0p + 'ENTER INITIAL INDEX (CHANNEL) NUMBER '
[6]  'ENTER DATA (PUT ONLY 0 ON A LINE IN ORDER TO STOP) (TYPE 'SAME' TO REUSE LAST DATA)'
[7]  SAME+Y
[8]  Y+10
[9]  LOOP2:ENTRY+
[10]  +(ENTRY^. =0)/LABEL2
[11]  Y+Y,ENTRY
[12]  +LOOP2
[13]  A REQUEST PRINT INSTRUCTIONS
[14]  LABEL2: + 'PRINT RAW DATA? (ENTER Y OR N) '
[15]  ANS+32+
[16]  +((YES^NO),(YES+^/ANS='Y'),(NO+^/ANS='N'))/LABEL2,LABEL3,LABEL5
[17]  A COUNT ROWS, LABEL, AND FORMAT THE OUTPUT
[18]  LABEL3:ROWS+(+10)*(10+(HIROW+10*(LAST+INIT+(pY)+^1)+10)-(LOROW+10*(FIRST+INIT)+10))
[19]  INDEX+LOROW+^10+10*ROWS
[20]  M+(0,10p1)\(ROWS,10)p((FIRST-LOROW)p0),Y,(HIROW+9-LAST)p0
[21]  M[1]+INDEX
[22]  4 1 p ' '
[23]  'RAW DATA'
[24]  (4 0 12 1 ,18p 10 1) DFT M
[25]  4 1 p ' '
[26]  A REQUEST FOR CORRECTIONS
[27]  LABEL5: + 'ANY CORRECTIONS? (ENTER Y OR N) '
[28]  ANS+33+
[29]  +((YES^NO),(YES+^/ANS='Y'),(NO+^/ANS='N'))/LABEL5,LABEL6,0
[30]  A ENTER CORRECTIONS
[31]  LABEL6: '5 TYPES OF CORRECTIONS:1) CHANGE INITIAL CHANNEL
      2) CHANGE SPECIFIC VALUE(S)
      3) OBLITERATE VALUE(S), CLOSEUP
      4) CREATE BLANK(S), EXPAND
      5) CONTINUE ADDING DATA'
[32]  LABEL1: 'ENTER 1 2 3 4 OR 5'
[33]  TYPE+
[34]  +(TYPE= 1 2 3 4 5)/LABEL7,LABEL8,LABEL9,LABEL10,LOOP2
[35]  +LABEL1
[36]  LABEL7: 'ENTER INITIAL INDEX (CHANNEL) NUMBER.'
[37]  INIT+
[38]  +LABEL2
[39]  LABEL8: 'ENTER CORRECTIONS AS PAIRS OF NUMBERS WITH THE CHANNEL NUMBER FIRST THEN DATA,E.G.,'
[40]  '178 22654 179 22690 211 10420'
[41]  CORR+10
[42]  'PUT ONLY 0 ON A LINE IN ORDER TO STOP.'
[43]  LOOP3:NEW+
[44]  +(NEW^. =0)/ENTER
[45]  CORR+CORR,NEW
[46]  +LOOP3
[47]  ENTER:DATA+CORR[EVEN+2*(1(pCORR)+2)]
[48]  CHAN+CORR[EVEN-1]
[49]  Y[CHAN+1-INIT]+DATA
[50]  +LABEL2
[51]  LABEL9: 'ENTER CHANNEL NUMBER(S) OF VALUE(S) TO BE OBLITERATED,E.G., 16 17 18'
[52]  OBLIT+
[53]  Y+(~(((INIT-1)+1pY)eOBLIT))/Y
[54]  +LABEL2
[55]  LABEL10: 'ENTER PRESENT NUMBERS OF EACH CHANNEL TO BE FOLLOWED BY A BLANK.'
[56]  'REPEAT ENTRY FOR MULTIPLE BLANKS.'
[57]  PAD+
[58]  LIST+PAD,(INIT-1)+1pY
[59]  PADDED+LIST[LIST]
[60]  Y+(~PADDED=((*1),^1+PADDED))\Y
[61]  +LABEL2
V

```

```

VGFIT[ ]V
V GFIT;ANS;C;CC;COEF;COV;D;DIFF;E;F;FWHM;G;H;I;INTEN;K;L;LIM;M;N;NEW;NU;OLD;P;POLY;S2;T;T1;VAR;
W;WT;X
[1]  * THIS PROGRAM FITS INPUT DATA USING GAUSSIAN PEAKS ON A POLYNOMIAL BACKGROUND.
[2]  * DATA IS WEIGHTED USING POISSON STATISTICS.
[3]  * REQUIRES BSP, INPUT, AND DFT.
[4]  * ENTER DATA
[5]  START:INPUT
[6]  * ENTER CONSTANTS AND GUESSES
[7]  CONST:D=0,OP=0 'DEGREE OF BACKGROUND POLYNOMIAL?'
[8]  WT=0,OP=0 'TYPE 0 FOR NO WEIGHTS, 1 FOR POISSON WEIGHTS'
[9]  K=0,OP=0 'ITERATION INCREMENT FRACTION? (0<K<1)'
[10] LIM=0,OP=0 'MAXIMUM ITERATIONS BETWEEN STATUS REPORTS?'
[11] P=0,OP=0 'APPROXIMATE PEAK POSITIONS?'
[12] W=(+1.6651)*FWHM+0,OP=0 'APPROXIMATE PEAK FWHM?'
[13] * INITIALIZE MISC. VALUES
[14] T1=1
[15] N=1+1+D
[16] NEW=(N+3*OP)P
[17] X=INIT+(1*P)-1
[18] E=X*.*(-1+1/N)
[19] INTEN=(OP)P
[20] * BEGIN ITERATION LOOP
[21] CONTINUE:T=0
[22] ITERATE:=(LIM<T+1)/STATUS
[23] T1=T1+1
[24] I=((OP)P).*INTEN
[25] F=(M*(O1)*0.5)**-((L+X*. -P)*M+((OP)P).*W)*2
[26] G=I*F*M*(2*(L*M)*2)-1
[27] H=I*F*2*L*M*2
[28] L=M+0
[29] C=E,F,G,H
[30] G=H+0
[31] -(T1>1)/SOLVE
[32] * ESTIMATE INTENSITY ON FIRST PASS
[33] -(WT=1)/3+I26
[34] COEF=(R(QC)+.X C)+.X(QC)+.X Y
[35] +2+I26
[36] COEF=(R(QC)+.X C+(Y+0=Y).*(-1+OP)P)+.X+/QC
[37] C=0
[38] INTEN=(OP)+N+COEF
[39] W=W+((OP)+(N+OP)+COEF)+INTEN
[40] P=P+((OP)+(N+2*OP)+COEF)+INTEN
[41] ->CONTINUE
[42] SOLVE:-(WT=1)/3+I26
[43] COEF=(CC+R(QC)+.X C)+.X(QC)+.X Y-+/I*F
[44] +2+I26
[45] COEF=(CC+R(QC)+.X C+(Y+0=Y).*(-1+OP)P)+.X(+/QC)-(QC)+.X(+/I*F)+Y+0=Y
[46] C=0
[47] * FORM ANSWER FROM SOLUTION VECTOR COEF
[48] POLY=N+COEF
[49] INTEN=INTEN+(OP)+N+COEF
[50] FWHM=((O16)*0.5)*W+W+(OP)+(N+OP)+COEF
[51] P=P+(OP)+(N+2*OP)+COEF
[52] OLD=NEW
[53] NEW=POLY,INTEN,W,P
[54] * TEST IF CHANGES ARE SIGNIFICANT
[55] -(V/(|(OLD-NEW)+OLD)>0.001)/ITERATE
[56] * COMPUTE VARIANCE
[57] DIFF=Y-(E+.X POLY)++/I*F
[58] S2=(DIFF+.X DIFF+Y+0=Y)+NU+(OP)-OP COEF
[59] VAR=(1 1 Q(CC*S2))*0.5
[60] VAR=VAR*((N+OP)P),((OP)P(O16)*0.5),((OP)P
[61] * FINAL ANSWER TABULATION
[62] 1 1 P '
[63] TABLE:'AFTER 'T1;' ITERATIONS:'
[64] POM+((OP),4)P ' +',RSP,'-'
[65] SUB+(4+18),(14),(29+18),(12+18),(14),(37+18),(20+19),(14),(45+19)
[66] ' INTENSITY WIDTH POSITION'
[67] (POM,(8 1 8 2 9 2 8 2 8 3 9 3) DFTQ(6,(OP)P(INTEN,FWHM,P,N+VAR)))[;SUB]
[68] 1 1 P '
[69] 'POLYNOMIAL COEFFICIENTS STARTING WITH CONSTANT ARE:'
[70] POM+(N,4)P ' +',RSP,'-'
[71] SUB+(4+110),(14),(14+11)
[72] (POM,(10 4 11 5) DFTQ(2,N)P(POLY,N+VAR)))[;SUB]
[73] 1 1 P '
[74] -END
[75] * STATUS REPORT
[76] STATUS:T1;' ITERATIONS; CHANGES > 0.1 PERCENT. I, FWHM, AND POSITION ARE 'INTEN,FWHM,P
[77] 'MORE ITERATIONS? (Y OR N)'
[78] ANS=0
[79] -(^/ANS='Y')/CONTINUE
[80] END:ANS=0,OP=0 'ANOTHER SET OF DATA? (Y OR N)'
[81] -(^/ANS='Y')/START
[82] +0,OP=0 'END'
V

```

GFIT
 ENTER INITIAL INDEX (CHANNEL) NUMBER 168
 ENTER DATA (PUT ONLY 0 ON A LINE IN ORDER TO STOP) (TYPE 'SAME' TO REUSE LAST Y VALUE)
:
 SAME
:
 0
 PRINT RAW DATA? (ENTER Y OR N) Y

RAW DATA

160	0.0	0.0	0.0	0.0	0.0	0.0	0.0	0.0	2.0	3.0
170	5.0	4.0	7.0	8.0	3.0	7.0	9.0	9.0	9.0	26.0
180	30.0	51.0	66.0	100.0	87.0	98.0	114.0	147.0	131.0	141.0
190	129.0	115.0	97.0	71.0	61.0	55.0	33.0	29.0	17.0	15.0
200	10.0	13.0	10.0	7.0	11.0	7.0	10.0	8.0	11.0	21.0
210	26.0	37.0	39.0	62.0	85.0	102.0	101.0	118.0	115.0	126.0
220	128.0	110.0	95.0	90.0	76.0	60.0	44.0	37.0	22.0	18.0
230	23.0	9.0	7.0	6.0	6.0	3.0	5.0	4.0	3.0	2.0

ANY CORRECTIONS? (ENTER Y OR N) Y
 5 TYPES OF CORRECTIONS: 1) CHANGE INITIAL CHANNEL
 2) CHANGE SPECIFIC VALUE(S)
 3) OBLITERATE VALUE(S), CLOSEUP
 4) CREATE BLANK(S), EXPAND
 5) CONTINUE ADDING DATA

ENTER 1 2 3 4 OR 5

:
 2
 ENTER CORRECTIONS AS PAIRS OF NUMBERS WITH THE CHANNEL NUMBER FIRST THEN DATA, E.G.,
 178 22654 179 22690 211 10420
 PUT ONLY 0 ON A LINE IN ORDER TO STOP.

:
 239 3

:
 0
 PRINT RAW DATA? (ENTER Y OR N) N
 ANY CORRECTIONS? (ENTER Y OR N) N
 DEGREE OF BACKGROUND POLYNOMIAL? 0
 TYPE 0 FOR NO WEIGHTS, 1 FOR POISSON WEIGHTS 1
 ITERATION INCREMENT FRACTION? (0<K<1) 1
 MAXIMUM ITERATIONS BEFORE STATUS REPORT? 3
 APPROXIMATE PEAK POSITIONS? 188 218
 APPROXIMATE PEAK FWHM? 12 12

AFTER 3 ITERATIONS:
 INTENSITY

INTENSITY	WIDTH	POSITION
1548.4 ± 38.31	10.98 ± 0.233	188.19 ± 0.115
1474.7 ± 37.77	11.54 ± 0.258	218.93 ± 0.120

POLYNOMIAL COEFFICIENTS STARTING WITH CONSTANT ARE:

3.7886 ± 0.45400

ANOTHER SET OF DATA? (Y OR N) N
 END

VSMOOTH []V

```
V SMOOTH;ALL;ANS;CHEB;C1;C2;D;DEN;DERIV;E;F;FIRST;HIROW;I;INDEX;LAST;LOROW;M;MATNORM;N;NO;NORM;
P;PT;ROWS;V;W;W1;YES
[1]  * THIS PROGRAM SMOOTHS OR DIFFERENTIATES PHA DATA BY FITTING A LEAST SQUARES
[2]  * POLYNOMIAL TO SUCCESSIVE SMALL REGIONS. ONLY THE MIDPOINT IS EVALUATED FOR EACH FIT.
[3]  * REQUIRES INPUT, CSTN, CSTV, Y, AND DFT.
[4]  START:INPUT
[5]  * ENTER_INITIAL_CONSTANTS
[6]  LABEL4:'INPUT NUMBER OF POINTS FITTED AT ONE TIME (PICK QDD NUMBER ≥3)'
[7]  P+□
[8]  'INPUT DEGREE OF POLYNOMIAL (';(1(P-1));)''
[9]  D+□
[10] 'ENTER DEGREE OF DERIVATIVE DESIRED (';(-1+(D+1));)'. 0TH DERIVATIVE GIVES SMOOTHING.'
[11] DERIV+□
[12] * COMPUTE_WEIGHTS_W
[13] CHEB+((D+1),(D+1))ρ0
[14] CHEB[1;]+1,Dρ0
[15] CHEB[2;]+0,(-2+(P-1)),(D-1)ρ0
[16] N+1
[17] LOOP1:→(D<N+N+1)/LABEL1
[18] C1+(2-4×N)+DEN+N×P-N
[19] C2+(1-N)×(P+N-1)+DEN
[20] CHEB[N+1;]+(C1×-1φCHEB[N;])+C2×CHEB[N-1;]
[21] →LOOP1
[22] LABEL1:W1+Q((1P)-(P+1)+2)○.×(-1+(D+1))
[23] F+CHEB+.×W1
[24] NORM+÷F*2
[25] MATNORM+NORM○.×Pρ1
[26] PT+F+MATNORM
[27] E+(1(D+1))=(D+1)ρ(DERIV+1)
[28] W+,W+E+.×ALL+(!(-1+(D+1))○.×Pρ1)×(φCHEB)+.×PT
[29] * COMPUTE_WEIGHTED_AVERAGE
[30] V+I+0
[31] LOOP2:→((ρW)<I+I+1)/LABEL2
[32] V+V+W[I]×Y[(I-1)+1(ρY)+1-ρW]
[33] →LOOP2
[34] *COUNT_ROWS,_LABEL,_AND_FORMAT_THE_OUTPUT
[35] LABEL2:ROWS+(+10)×(10+(HIROW+10×[(LAST+INIT+(ρV)-1-(P-1)+2)+10)-(LOROW+10×[(FIRST+INIT+(P-1)+
2)+10]))
[36] INDEX+LOROW+-110+10×\ROWS
[37] M+(0,10ρ1)\(ROWS,10)ρ((FIRST-LOROW)ρ0),V,(HIROW+9-LAST)ρ0
[38] M[;1]+INDEX
[39] 4 1 ρ' '
[40] P;' POINTS; DEGREE 'D;' POLYNOMIAL; 'DERIV;' ORDER DERIVATIVE.'
[41] (4 0 12 1 ,18ρ 10 1) DFT M
[42] 4 1 ρ' '
[43] LABEL7:'TRY DIFFERENT FIT? (ENTER Y OR N)'
[44] ANS+□
[45] +((YES≠NO),(YES+^/ANS='Y'),(NO+^/ANS='N'))/LABEL7,LABEL4,LABEL8
[46] LABEL8:'NEW SPECTRUM? (ENTER Y OR N)'
[47] ANS+□
[48] +((YES≠NO),(YES+^/ANS='Y'),(NO+^/ANS='N'))/LABEL8,START,LABEL10
[49] LABEL10:→0,ρ□+'END'
```

SMOOTH
ENTER INITIAL INDEX (CHANNEL) NUMBER

: 1
ENTER DATA (PUT ONLY 0 ON A LINE IN ORDER TO STOP) (TYPE 'SAME' TO REUSE LAST Y VALUE)
: SAME
: 0
PRINT RAW DATA? (ENTER Y OR N)
Y

RAW DATA

0	0.0	0.0	0.1	0.0	0.3	0.3	0.5	11.2	23.1	45.2
10	48.0	56.2	56.9	25.2	13.6	10.0	4.5	-1.5	0.1	-0.3
20	-0.0	0.0	0.0	0.0	0.0	0.0.	0.0	0.0	0.0	0.0

ANY CORRECTIONS? (ENTER Y OR N)

N
INPUT NUMBER OF POINTS FITTED AT ONE TIME (PICK QDD NUMBER ≥ 3)

: 5
INPUT DEGREE OF POLYNOMIAL (≤ 4)

: 2
ENTER DEGREE OF DERIVATIVE DESIRED (0 1 2), 0TH DERIVATIVE GIVES SMOOTHING.

: 0
RAW DATA IS STORED AS GLOBAL VARIABLES Y AND X.
COMPUTED DATA IS STORED AS GLOBAL VARIABLES YY AND XX.
PRINT COMPUTED DATA? (Y OR N)
Y

5 POINTS PER FIT; DEGREE 2 POLYNOMIAL; 0 ORDER DERIVATIVE.

0	0.0	0.0	0.0	0.1	0.2	-0.6	2.2	9.6	26.4	40.6
10	51.2	57.2	50.3	30.7	13.4	9.0	4.0	0.1	-0.9	0.0

TRY DIFFERENT FIT? (ENTER Y OR N)

N
NEW SPECTRUM? (ENTER Y OR N)
N
END

```

VPROFILE[ ]V
V PROFILE;ANGLE;PHI;D;GAS;SUB;MU;ALLMU;RHO;ALLRHO;P;W;FWHM;SIGMA;XSPAN;INIT;S;R;T;F;A;ANS;B;C
[1] * THIS PROGRAM GENERATES THE CHARGE DISTRIBUTION AT THE ANODE WIRE FOR PHOTONS INCIDENT ON A SLANT
[2] * ENTER VARIABLE PARAMETERS
[3] * ENTER DIAMETER (THICKNESS) OF THE COUNTER IN CM.'
[4] D+
[5] * ENTER THE NAME OF THE GAS (NEON, ARGON, KRYPTON, XENON).'
[6] SUB+'NAXX'\1+GAS+
[7] +(SUB=5)/6
[8] MU+(ALLMU+ 54.3 285 237.8 726.1)[SUB]
[9] RHO+(ALLRHO+ 0.0009 0.00178 0.00371 0.00585)[SUB]
[10] * ENTER ANGLE(S) BETWEEN THE INCIDENT PHOTON AND ANODE WIRE IN DEGREES.'
[11] ANGLE+(PHI+, )+180
[12] * ENTER THE PRESSURE(S) IN ATMOSPHERES.
[13] P+,
[14] * ESTABLISH SYSTEM CONSTANTS (IN EQUIVALENT CM).
[15] RNG+(ALLRNG+ 0.000115 4.6E-5 9E-5 1.2E-5)[SUB]
[16] NOISE+0.025
[17] INH+RNG+P*RHO
[18] SLIT+0.022
[19] W+(+1.6651)*FWHM+((NOISE*2)+(INH*2)+(SLIT*2))*0.5
[20] SIGMA+MU*RHO*P
[21] * DETERMINE X SCALE
[22] * RETAIN SAME X SCALE AS IN LAST PLOT? (Y OR N)'
[23] ANS1+
[24] +(ANS1='Y')/3+I26
[25] * USE SAME X SCALE ON ALL PLOTS?'
[26] ANS2+
[27] * CHANGE TO PLOT BALL; GIVE CARRIAGE RETURN WHEN READY.'
[28] A+
[29] * CALCULATE DISTRIBUTION
[30] J+1
[31] JLOOP:I+1
[32] ILOOP:+(ANS1='Y')/ENDX
[33] XSPAN+(10*W[J])+(D+3*ANGLE[I])L4+SIGMA[J]
[34] INIT+-5*W[J]
[35] X+INIT,INIT+(XSPAN+60)*.160
[36] ANS1+ANS2
[37] ENDX:+(PHI[I]=90)/NORMAL
[38] S+(X+W[J])-R+W[J]*SIGMA[J]+2*2*ANGLE[I]
[39] T+D+W[J]*3*ANGLE[I]
[40] F+SIGMA[J]*(+R*2)*(-X*SIGMA[J]+2*ANGLE[I])*((B+ERF T-S)-C+ERF-S)+2*2*ANGLE[I]
[41] F+F*~(1E-5>1-B)^(1E-5>1-C)
[42] +2+I26
[43] NORMAL:F+(1+-SIGMA[J]*D)*(-X+W[J])*2+W[J]*(O1)*0.5
[44] * PLOT DATA
[45] XAXIS+'POSITION (CM)'
[46] YAXIS+'INTENSITY'
[47] TITLE1+45+GAS,' GAS AT ',(3 1 DFT P[J]),' ATMOSPHERE PRESSURE.'
[48] TITLE2+45+'ANGLE BETWEEN TRACK AND WIRE IS ',(4 1 DFT PHI[I]),' DEGREES.'
[49] TITLE3+45+'(FWHM AT 90 DEG WOULD BE ',(4 2 DFT FWHM[J]*10),' MM).'
[50] TITLE+ 3 45 P TITLE1,TITLE2,TITLE3
[51] 2 1 P ' '
[52] B PLOT
[53] 3 1 P ' '
[54] +((P ANGLE)≥I+I+1)/ILOOP
[55] +((P P)≥J+J+1)/JLOOP
[56] +0
V

```

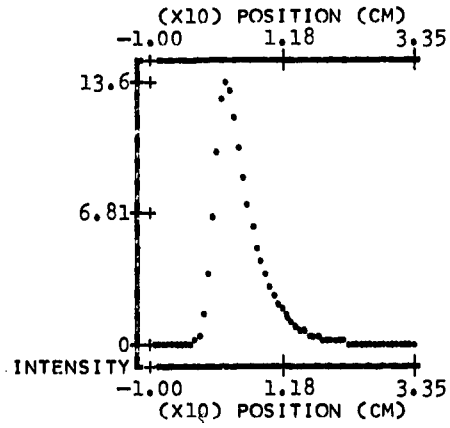
```

VB PLOT[ ]V
V B PLOT;W;D
[1] A+
[2] 2 1 2 A PLOT .F VS X
V

```

PROFILE
 ENTER DIAMETER (THICKNESS) OF THE COUNTER IN CM.
 □: 1.27
 ENTER THE NAME OF THE GAS (NEON, ARGON, KRYPTON, XENON).
 XENON
 ENTER ANGLE(S) BETWEEN THE INCIDENT PHOTON AND ANODE WIRE IN DEGREES.
 □: 45
 ENTER THE PRESSURE(S) IN ATMOSPHERES.
 □: 4
 RETAIN SAME X SCALE AS IN LAST PLOT? (Y OR N)
 N
 USE SAME X SCALE ON ALL PLOTS?
 Y
 CHANGE TO PLOT BALL; GIVE CARRIAGE RETURN WHEN READY.

XENON GAS AT 4.0 ATMOSPHERE PRESSURE.
 ANGLE BETWEEN TRACK AND WIRE IS 45.0 DEGREES.
 (FWHM AT 90 DEG WOULD BE 0.33 MM).



24